

# Exploring a Yield Curve Inspired Generalization of Correlation in the Extended SSVI Model

Zachary Polaski

This Draft: July 15, 2023

## **Abstract:**

**This paper explores whether an extension to the SSVI model of the implied volatility surface that aims to capture the behavior inferred from maturity-specific calibrations of existing parameterizations can offer performance improvements while satisfying the necessary no-arbitrage constraints. It is found that although a functional form for the correlation between the underlying asset and its instantaneous volatility that more suitably reflects the oscillatory behavior implied by the maturity-wise calibrations can be found by a generalization of the extended SSVI (eSSVI) model, the no-arbitrage constraints prove too restrictive to allow admissible parameterizations that take advantage of the offered flexibility.**

**Keywords:** Option Pricing, Implied Volatility Modeling, SSVI, Arbitrage.

# Contents

<b>1</b>	<b>Introduction</b>	<b>1</b>
refsection0		
1.1	Motivations and Literature Review . . . . .	1
refsection0		
1.2	Organization of Paper . . . . .	2
refsecti0n0	<b>Model Setup</b>	<b>3</b>
refsection0		
2.1	European Options . . . . .	3
refsection0		
2.2	The Black-Scholes Model . . . . .	4
refsection0		
2.2.1	Implied Volatility . . . . .	5
refsection0		
2.2.2	Arbitrage . . . . .	7
refsecti0n0	<b>Parameterizing the Implied Volatility Surface</b>	<b>14</b>
refsection0		
3.1	Gatheral's and Jacquier's SVI and SSVI . . . . .	14
refsection0		
3.1.1	The SVI Model . . . . .	14
refsection0		
3.1.2	Absence of Arbitrage in the SVI Model . . . . .	14
refsection0		
3.1.3	The SSVI Model . . . . .	15
refsection0		
3.1.4	Absence of Arbitrage in the SSVI Model . . . . .	15
refsection0		
3.2	Hendricks' and Martini's eSSVI . . . . .	19
refsection0		
3.2.1	Absence of Arbitrage in the eSSVI Model . . . . .	19
refsecti0n0	<b>Model Calibrations</b>	<b>20</b>
refsection0		
4.1	Risk-Neutral Calibration Methodology . . . . .	20
refsection0		
4.2	Market Data and Input Assumptions . . . . .	21
refsection0		
4.3	Choice of Functional Forms for $\varphi$ and $\rho$ . . . . .	22
refsection0		

4.4 Calibration Results for SSVI and eSSVI Models . . . . .	23
refsection0	
4.4.1 SSVI Explicit No Arbitrage Conditions . . . . .	23
refsection0	
4.4.2 SSVI Calibration Results . . . . .	24
refsection0	
4.4.3 eSSVI Explicit No Arbitrage Conditions . . . . .	26
refsection0	
4.4.4 eSSVI Calibration Results . . . . .	27
refsecti <b>5</b> n0 <b>Generalizing the Functional Form for Correlation</b>	30
refsection0	
5.1 Motivation . . . . .	30
refsection0	
5.2 The RxSSVI Model . . . . .	35
refsection0	
5.3 No-Arbitrage Conditions . . . . .	36
refsection0	
5.4 Calibration Results for Rx Models . . . . .	37
refsection0	
5.4.1 R1 Model . . . . .	39
refsection0	
5.4.2 R2 Model . . . . .	42
refsection0	
5.4.3 R3 Model . . . . .	45
refsecti <b>6</b> n0 <b>Conclusion</b>	48
refsecti <b>R</b> eferences	49
refsecti <b>A</b> ppendices	52
refsecti <b>A</b> n0 <b>The Black-Scholes Model</b>	52
refsection0	
A.1 Derivation of the PDE for a Non-Dividend Paying Asset . . . . .	52
refsection0	
A.2 Change of Measure for a Non-Dividend Paying Asset . . . . .	55
refsection0	
A.3 Solution to the Stochastic Dynamics of a Non-Dividend Paying Asset . . . . .	59
refsection0	

# 1 Introduction

## 1.1 Motivations and Literature Review

This paper undertakes the development of a model of the implied volatility surface. The research builds mainly off of the results and methodology of [**Gatheral and Jacquier 2013**] and [**Hendricks and Martini 2019**], the latter of which provided an extension to the pioneering framework of the former, and which becomes a special case of the more generalized extension developed herein.

The use and study of European-style options is indeed old. For instance, in [**Nelson 1904**] and [**Higgins 1906**], one may be surprised to find that traders in 19th century New York and London were already employing rules-of-thumb to value and hedge these contracts (such as selling half of the underlying to hedge the writing of an at-the-money call) which would later prove to be approximations to the analytical solutions formalized nearly a century later. Of these modern analytical formalizations, the most important is undoubtedly the Black-Scholes framework of Fischer Black and Myron Scholes, introduced in the beyond-seminal paper "The Pricing of Options and Corporate Liabilities" [**Black and Scholes 1973**]. Even still, the use of advanced mathematics in the study of finance, in particular the Brownian motion as a source of randomness, dates back to the PhD thesis of Louis Bachelier, "Théorie de la Spéculation," published in 1900 ([**Bachelier 1900**]). The work was wildly under-appreciated due to the rigidity of the French mathematical community of the time and wouldn't receive any further consideration for decades. Throughout the 1970s and 1980s, the shortcomings of the Black-Scholes model became all too apparent, particularly in the aftermath of the events of October 19th, 1987, now known as "Black Monday," which saw a permanent regime change in the implied volatility structure that the Black-Scholes model simply could not handle. This new stylized feature, to become widely known as the "volatility smile," implying that market participants placed a meaningfully higher probability on extreme returns than implied by a normal distribution, would become the focus of academics and practitioners working to build realistic models to price and hedge increasingly complicated financial products, with the Black-Scholes model relegated (though still invaluable) to simply a tool to map implied volatilities back to prices. Initially, and still to a large degree, such research focused on improved assumptions and models for the stochastic dynamics of the underlying asset. A particularly appealing class of models emerged known as stochastic volatility models, which addressed the problem rather directly by making the variance of the underlying stochastic process itself a stochastic process. Such models include the CEV model of [**Cox 1975**] and the SABR model of [**Hagan et. al. 2002**], although the most popular and still widely used stochastic volatility model is certainly the Heston model of [**Heston 1993**]. Other approaches would skirt the normality assumption through the introduction of discontinuities in the underlying sample paths. For instance, in [**Merton 1976**], Poisson-distributed jumps

were added to a continuous diffusion, although the initial motivation for this extension was to relax the assumption that the underlying stochastic process had strictly continuous sample paths rather than to produce market-consistent implied volatility. This introduction of discontinuities or jumps in the evolution of asset prices would eventually culminate in the application of Lévy processes, which offer a very flexible generalization of stochastic processes, of which the Brownian motion is a special case. In [**Madan and Seneta 1990**] much of the current framework for using Lévy processes for price modeling was first developed with the Variance Gamma (VG) process, although the idea of modeling prices with infinite activity discontinuities had already been considered years earlier in [**Mandelbrot 1963**], [**Press 1967**], [**Praetz 1972**], and [**Bookstaber 1987**]. Since the Variance Gamma process, a number of additional Lévy processes have been proposed to more realistically capture stylized facts of the markets, perhaps the most popular being the Hyperbolic process of [**Eberlein 1995**], the Normal Inverse Gaussian process of [**Barndorff-Nielsen 1995**], the CGMY process of [**Carr et. al. 2002**], the Kou process of [**Kou 2002**], and the Meixner process of [**Schoutens 2001**].

Rather than beginning with an assumption for the underlying stochastic dynamics, [**Gatheral 2004**] took a more direct approach to modeling the volatility surface by doing just that - modeling the volatility surface. Unfortunately, this early attempt has proven computationally uncooperative and it is difficult or impossible to ensure that arbitrage is not admitted by the model. In [**Gatheral and Jacquier 2013**], a significant advancement was made in developing a time-dependent version of this model that could fit any number of maturities with a single parameterization. The true utility of this model, however, was the ability to derive clear conditions to prevent arbitrage across the entire implied volatility surface. However, the parsimony of this model left much to be desired in the way of calibration error, and in [**Hendricks and Martini 2019**] the authors began exploring ways to extend the model to address this concern. It is from here that this paper picks up, in the study of a generalization of this most recent extension.

## 1.2 Organization of Paper

The paper will be organized as follows. Section 2 will introduce some basic concepts regarding option pricing. In addition to payoffs and arbitrage, the Black-Scholes model and its association with implied volatility will also importantly be introduced here. Section 3 will review existing models for the implied volatility surface, which include the SVI and SSVI models. The recent extension to the SSVI model, the eSSVI model will also be introduced here, which serves as the main inspiration and reference for the model developed herein. Section 4 details how the models will be calibrated to real-world option price data as a means to assess the relative performance of the various models. In this section calibration results for the SSVI and eSSVI model will also be presented. Section 5 introduces the main contribution of this paper, which is the study of a generalization of the eSSVI model. Motivation for the extension, relevant no-arbitrage constraints, and calibration results will all be discussed in this section. Section 6 concludes.

## 2 Model Setup

### 2.1 European Options

We begin with some basic definitions and descriptions of the types of financial assets which will be the subject of this study. In particular, the assets under study are *financial derivatives*, also known as *contingent claims* due to the fact that their value is contingent upon the evolution of some underlying or reference asset.

**Definition 2.1** A *contingent claim* is a stochastic variable of the form

$$X = \Phi(S_T), \quad (2.1)$$

where the contract or payoff function  $\Phi$  is some real-valued function of underlying asset  $S$  at future time  $T$ .

The simplest types of contingent claims are *European options*, which give the holder (writer) the right (obligation) to buy (sell) or sell (buy) the asset  $S$  at time  $T$  at a specified price  $K$  (called the "strike") agreed upon at time 0. Claims in which the writer has obliged to sell are called *call options*, and claims in which the writer has obliged to buy are called *put options*.

**Definition 2.2** A *European call option* is a contingent claim with payoff function to the holder

$$\Phi(S_T) = [S_T - K]^+. \quad (2.2)$$

**Definition 2.3** A *European put option* is a contingent claim with payoff function to the holder

$$\Phi(S_T) = [K - S_T]^+. \quad (2.3)$$

The nature of these payoffs leads to the concept of the *moneyness* of the option. A European call option is said to be *at-the-money (ATM)* when  $S_t = K, t \leq T$ , *out-of-the-money (OTM)* when  $S_t < K$ , and *in-the-money (ITM)* when  $S_t > K$ . Likewise, a European put option is said to be *at-the-money* when  $S_t = K$  (equivalent to the call condition), *out-of-the-money* when  $S_t > K$ , and *in-the-money* when  $S_t < K$ . In practice, when market participants speak of

"at-the-money" options, the description typically is not meant to hold with equality as above, and simply means that the underlying is trading arbitrarily near a particular strike.

## 2.2 The Black-Scholes Model

Under the Black-Scholes model, the risk-neutral dynamics<sup>1</sup> of the underlying asset  $S$  are governed by the lognormal process (known as a geometric Brownian motion),

$$dS_t = (r - q)S_t dt + \sigma S_t dW_t, \quad (2.4)$$

where  $S_t$  is the price of the underlying asset  $S$  at time  $t$ ,  $r$  is the continuously compounded risk-free interest rate from time  $t$  to  $T$ ,  $q$  is the continuously compounded dividend yield from time  $t$  to  $T$ ,  $\sigma$  is the annualized volatility (measured by the standard deviation of returns) of the underlying asset,  $dt$  is an arbitrarily small increment of time, and  $W_t$  is an increment of a Wiener process. The Black Scholes model admits analytical solutions for the prices of European options, with

$$C_{BS} = e^{-r(T-t)}[FN(d_1) - KN(d_2)]; \quad P_{BS} = e^{-r(T-t)}[KN(-d_2) - FN(-d_1)], \quad (2.5)$$

with  $C$  the value of a European call,  $P$  the value of a European put,  $N(\cdot)$  the standard normal cumulative distribution function, and

$$F = S_t e^{(r-q)(T-t)}, \quad (2.6)$$

$$d_1 = \frac{\ln(\frac{F}{K}) + \frac{1}{2}\sigma^2(T-t)}{\sigma\sqrt{T-t}}; \quad d_2 = d_1 - \sigma\sqrt{T-t}. \quad (2.7)$$

$F$  denotes the forward price of the underlying asset for time  $T$ , and casting the solution in terms of the forward is convenient as it allows one to more easily extend the solution for situations in which the underlying asset is assumed to pay discrete (typically more realistic for individual stocks and funds/ETFs) rather than proportional or continuous (typically only realistic for broad

---

<sup>1</sup>The notion of a risk-neutral measure is a subtle yet fundamental aspect of derivative pricing. For the interested reader, the classical treatment can be found in [Harrison and Pliska 1981]. Otherwise, it suffices to accept that the risk-neutral measure is a result of the assumption of a market free of arbitrage. For proof of this claim, as well as some additional proofs related to the Black-Scholes framework as presented here, see Appendix A.

indices) dividends. In these cases, we have

$$F = S_t e^{r(T-t)} - e^{r(T-t)} \sum_i^N D_i e^{-r_i(t_i-t)} \quad \forall t \leq t_i \leq T, \quad (2.8)$$

where  $t_i$  are the ex-dividend dates with corresponding discrete dividend  $D_i$  for the underlying asset  $S$ .

### 2.2.1 Implied Volatility

A significant limitation of the Black-Scholes model is the assumption of a constant volatility scalar  $\sigma$ . This assumption is equivalent to that of assuming log-normality of asset prices, which is further equivalent to the assumption of the normality of log returns, which has proven to be inconsistent with the true behavior of financial markets by an overwhelming amount of empirical evidence. The dynamics of Equation (2.4) are therefore unable to satisfactorily reproduce options quoted in the market, and when one inverts Equation (2.5) to solve for  $\sigma$  across an increasing vector of strikes  $K$  for any given tenor  $t$ , a typical pattern emerges known as a volatility smile or smirk. This inversion of Equation (2.5) for  $\sigma$  (which importantly does not have a known analytical solution and is rather found in practice using numerical methods) for a given strike and tenor is known as the *implied volatility* of the option for that particular strike and tenor. We will denote the Black-Scholes implied volatility for log forward moneyness  $k = \ln(\frac{K}{F})$  and tenor  $t$  by  $\sigma_{BS}(k, t)$ . It will also be useful later to think of Black-Scholes implied volatility in terms of total implied variance, which we will denote

$$\omega(k, t) = \sigma_{BS}^2(k, t)t. \quad (2.9)$$

While the Black-Scholes model is typically now deemed to be of little practical use given its many limiting assumptions, implied volatility offers a valuable means to uniquely quote option prices without referring to price (which will depend on the price magnitude of the underlying asset). Implied volatility may, in that sense, be thought of as the wrong number in the wrong model that reproduces the right price. The utility of this cannot be understated. By constructing a model which satisfactorily recreates the implied volatility surface of a given set of market quotes, related options without a ready market can be priced and hedged, such as FLEX options<sup>2</sup>

---

<sup>2</sup>FLEX options are non-standard or off-exchange options that allow both sides of the contract to negotiate various terms. For instance, a decimal strike may be negotiated, whereas exchange traded contracts typically only offer integer (or at most half-dollar) strikes. Naive interpolation of exchange traded quotes near the custom FLEX option strike may lead to problems such as arbitrage opportunities, thus facilitating the need for models consistent across an effective continuity of contract specifications.

or exotic payoffs on the same underlying. Figures 1 and 2 below show the implied volatility curves for SPX (S&P 500) options for a number of traded maturities on February 22nd, 2016. Notice that for short tenors, the implied volatility of options tends to increase as strike moves away from the money in either direction, but the increase is more acute as we move to lower strikes. For longer tenors, implied volatility is effectively monotonically decreasing in strike. This is the reason for the distinction of volatility "smirks" versus "smiles", with smirks being pervasive in markets for equity options of medium to long-term tenors and signaling that market participants place higher probabilities on extreme returns (and in particular extreme negative returns) than implied by a normal distribution. Note that when implied volatilities are plotted in three dimensions across both strikes and tenors, we typically speak of an implied volatility surface.

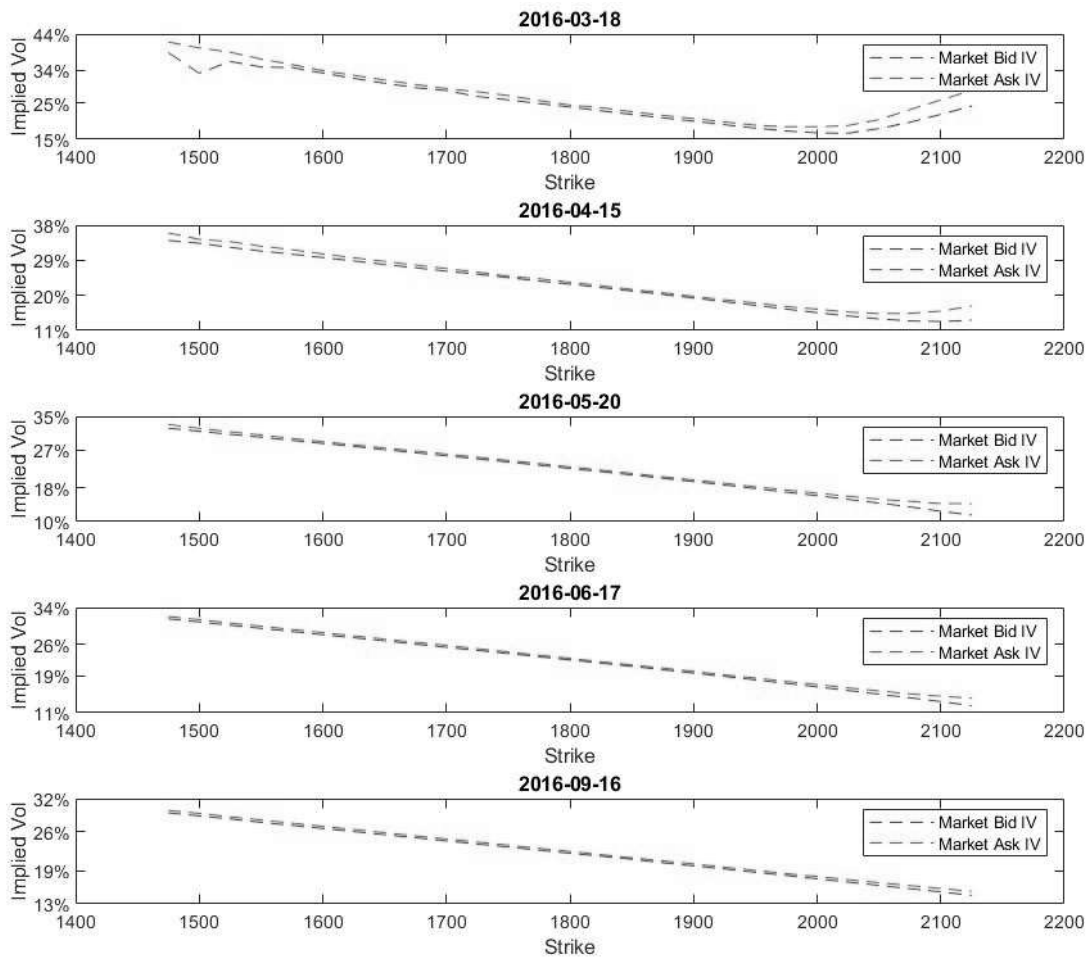


Figure 1: February 22nd, 2016 Market Implied Vols Set 1

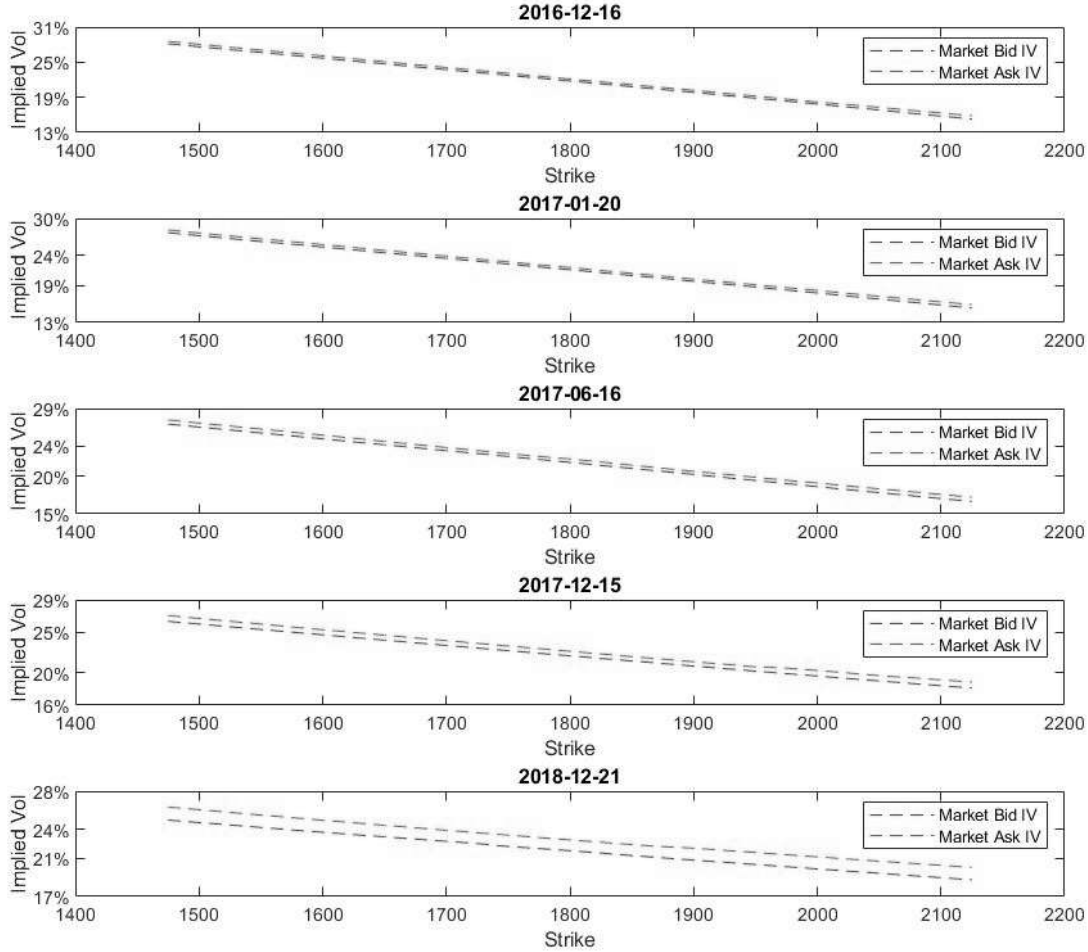


Figure 2: February 22nd, 2016 Market Implied Vols Set 2

### 2.2.2 Arbitrage

The absence of arbitrage, or riskless profits, is fundamental to option pricing. An arbitrage opportunity exists if a costless self-financing portfolio has zero probability of losing value but a positive probability of gaining value at time  $T$ . We formalize this idea with the following definition (see [Bjork 2009]).

**Definition 2.4** An *arbitrage portfolio*  $V^h$  is such that

$$V_0^h = 0; \quad \mathbb{P}(V_T^h \geq 0) = 1; \quad \mathbb{P}(V_T^h > 0) > 0 \quad (2.10)$$

As implied volatility offers a unique mapping to option prices (and the modeling of implied volatility will be the focus of this paper), it is useful to work with model-independent conditions for the absence of arbitrage on an implied volatility surface. In [**Carr and Madan 2005**], a volatility surface free of (static, or that which does not require rebalancing of the hedging portfolio) arbitrage is defined as follows.

**Definition 2.5** A volatility surface is free of static arbitrage if and only if:

- (i) it is free of calendar spread arbitrage;
- (ii) each time slice is free of butterfly arbitrage.

We can detail these conditions with some supporting lemmas, following closely [**Gatheral and Jacquier 2013**]. First, absence of calendar spread arbitrage implies the intuitive notion that option prices should be monotonically increasing in maturity. This condition can be expressed through total implied variance  $\omega(k, t)$  as follows.

**Lemma 2.1** A volatility surface is free of calendar spread arbitrage if:

$$\frac{\partial \omega(k, t)}{\partial t} \geq 0, \quad \forall k \in \mathbb{R}, t > 0, \quad (2.11)$$

*Proof.* Let  $\{X_n\}$  be a sub-martingale sequence, with  $a \geq 0$  and  $0 \leq t_1 \leq t_2$ . Define, for real numbers  $a, b, a \leq b$ ,  $U_n(a, b)$  as the number of upcrossings on the interval  $(a, b)$  that  $X$  completes by time  $n$ . Then by the sub-martingale upcrossing inequality, we have, for  $n = 1, 2, \dots$ ,

$$\mathbb{E}[U_n] \leq \frac{\mathbb{E}[(X_n - a)^+] - \mathbb{E}[(X_0 - a)^+]}{b - a}$$

$$\Leftrightarrow \underbrace{\mathbb{E}[U_n](b - a)}_{\geq 0} + \mathbb{E}[(X_0 - a)^+] \leq \mathbb{E}[(X_n - a)^+] \quad (2.12)$$

$$\implies \mathbb{E}[(X_0 - a)^+] \leq \mathbb{E}[(X_n - a)^+]. \quad (2.13)$$

Now, for any  $i \in n = 1, 2, \dots$ , let  $C_i$  be a call option with strike  $K_i$  and expiration  $t_i$ . Suppose

$$\frac{K_1}{F_1} = \frac{K_2}{F_2} = e^k, \quad (2.14)$$

then, given the risk-neutral dynamics of Equation(2.4), the process  $Y_t$  defined by  $Y_t := S_t/F_t$

for all  $t \geq 0, t \leq T$  is a martingale, as

$$\mathbb{E}\left[\frac{S_t}{F_t} = \frac{1}{F_t} S_0 e^{(r-q)T} = \frac{S_0}{F_0} = Y_0\right]. \quad (2.15)$$

Then, by Equation (2.13), we have

$$\mathbb{E}[(Y_{t_1} - e^k)^+] \leq \mathbb{E}[(Y_{t_2} - e^k)^+]. \quad (2.16)$$

So, keeping log moneyness  $e^k$  constant, option prices are non-decreasing in time to expiration. As the Black-Scholes solution can be written as  $C_{BS}(k, \omega(k, t))$  if  $C_{BS}$  is strictly increasing in its second argument, it must be that this second argument  $\omega(k, t)$  is likewise non-decreasing in its second argument  $t$ . To prove that  $C_{BS}$  is in fact non-decreasing in  $\omega(k, t)$ , note that the Black-Scholes solution for the price of a call option given in Equation (2.5) can be re-expressed as

$$C_{BS} = S(N(d_+) - e^k N(d_-)), \quad (2.17)$$

with

$$d_{\pm} = \frac{-k}{\sqrt{\omega(k)}} \pm \frac{\sqrt{\omega(k)}}{2}, \quad (2.18)$$

where we have for convenience dropped the dependence of  $\omega$  on  $t$  as we are now just considering any given tenor. Thus,

$$C_{BS} = S\left(N\left(\frac{-k}{\sqrt{\omega(k)}} + \frac{\sqrt{\omega(k)}}{2}\right) - e^k N\left(\frac{-k}{\sqrt{\omega(k)}} - \frac{\sqrt{\omega(k)}}{2}\right)\right). \quad (2.19)$$

Differentiating this with respect to  $\omega$  and simplifying yields

$$\frac{\partial C_{BS}}{\partial \omega} = \underbrace{SN'(d_+) \left[ \frac{1}{2\sqrt{\omega(k)}} \right]}_{\geq 0}, \quad (2.20)$$

with  $N'(\cdot)$  the standard normal probability density function. Note that this is analogous to Black-Scholes "vega," but in terms of total variance  $\omega$  rather than standard deviation  $\sigma$ . ■

Second, absence of butterfly spread arbitrage ensures the existence of a non-negative probability density. This is really no less intuitive than the notion of calendar spread arbitrage. Recall the famous result of [**Breeden and Litzenberger 1978**], which showed that the risk-neutral density of the underlying, which we will denote  $f(K)$ , can be computed from the prices of call options as

$$f(K) = e^{rT} \frac{\partial^2 C}{\partial K^2} \quad (2.21)$$

Thus, for the density  $f(K)$  to be valid, the second derivative of call prices with respect to strike must be non-negative everywhere (note that  $e^{rT}$  already satisfies this). Consider a second-order finite difference approximation of this derivative:

$$\frac{\partial^2 C}{\partial K^2} = \frac{C(K + \epsilon) - 2C(K) + C(K - \epsilon)}{\epsilon^2} \quad (2.22)$$

A trader can instantly recognize this as a butterfly spread strategy infinitesimally tight around  $K$ . It simply states that call prices, as functions of a convex payoff  $\Phi = [S_T - K]^+$ , are themselves convex in strike. Another way to present this is that option prices must satisfy Jensen's inequality, with

$$C(K) \leq \frac{1}{2}[C(K + \epsilon) + C(K - \epsilon)] \quad (2.23)$$

Figures 3 and 4 below show the mid price of traded SPX calls for a number of maturities on February 22nd, 2016 by strike.

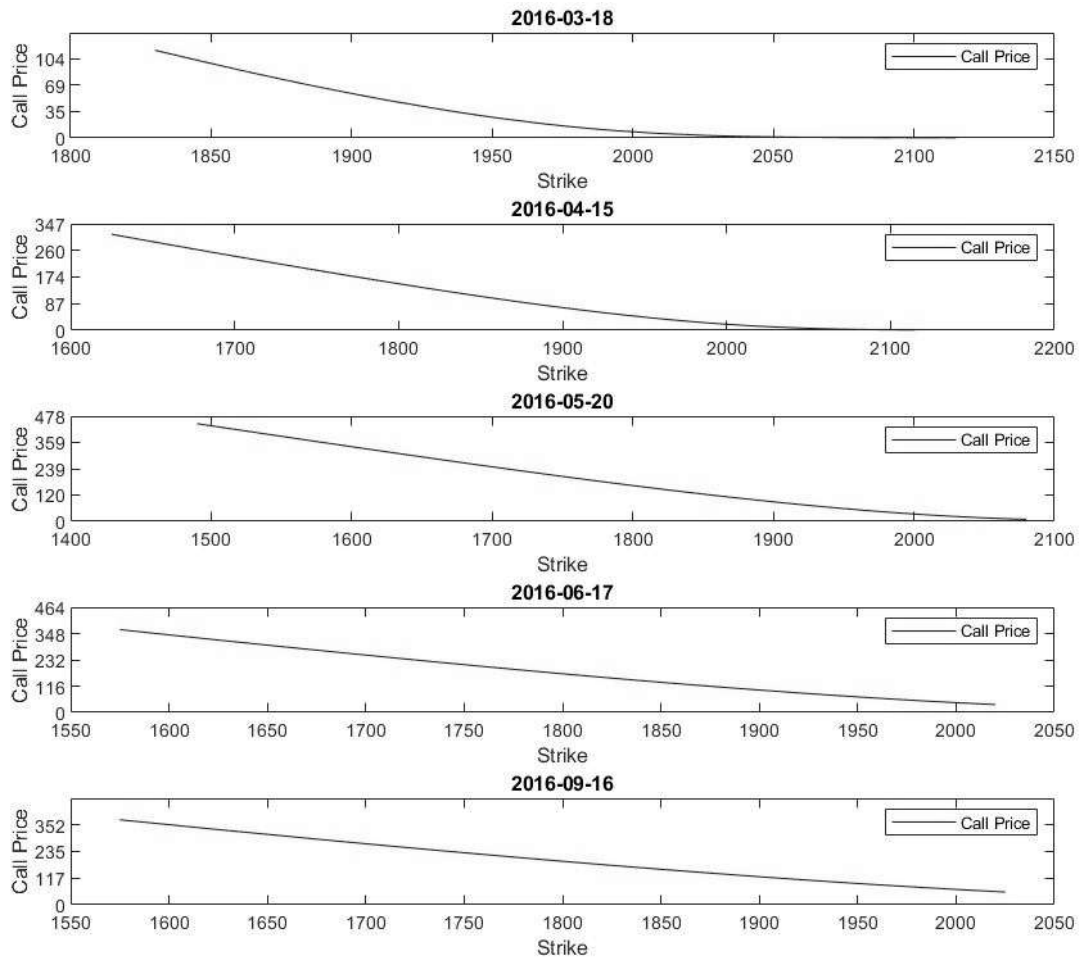


Figure 3: February 22nd, 2016 Market Call Prices Set 1

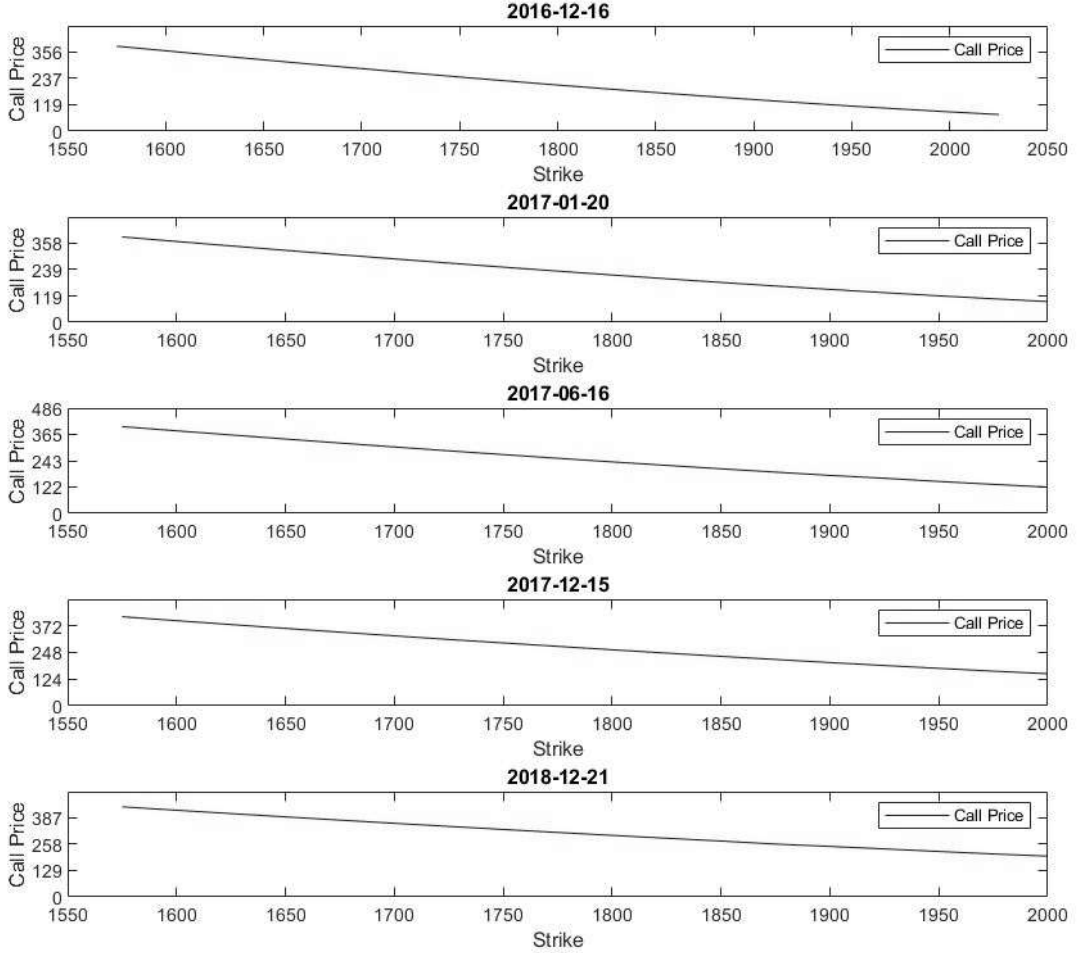


Figure 4: February 22nd, 2016 Market Call Prices Set 2

In [Gatheral and Jacquier 2013], this butterfly arbitrage condition is defined in terms of total implied variance  $\omega(k, t)$  as follows.

**Lemma 2.2** A volatility surface is free of butterfly spread arbitrage if and only if  $g(k) \geq 0 \forall k \in \mathbb{R}$  and  $\lim_{k \rightarrow +\infty} d_+(k) = -\infty$ , where:

$$g(k) := \left(1 - \frac{k \frac{\partial \omega(k)}{\partial k}}{2\omega(k)}\right)^2 - \frac{\frac{\partial \omega(k)}{\partial k}^2}{4} \left(\frac{1}{\omega(k)} + \frac{1}{4}\right) + \frac{\frac{\partial^2 \omega(k)}{\partial k^2}}{2}, \quad \text{and} \quad (2.24)$$

$$d_{\pm}(k) := -\frac{k}{\sqrt{\omega(k)}} \pm \frac{\sqrt{\omega(k)}}{2}. \quad (2.25)$$

*Proof.* By Equation (2.21), we know that the probability distribution implied by call option prices across strikes  $K$  of any tenor  $t$  is given by the second derivative of call option prices with respect to strike, accumulated at the risk-free rate. Noting that  $K = Fe^k$  and differentiating  $C_{BS}$  as given in Equation (2.19) twice with respect to this transformation yields

$$\frac{\partial^2 C_{BS}}{\partial(Fe^k)^2} = f(Fe^k) = \frac{g(k)}{Fe^k\sqrt{2\pi\omega(k)}}e^{-\frac{(d_-)^2}{2}}, \quad (2.26)$$

with  $g(k)$  as given in Equation (2.24). Given that the term

$$\frac{1}{Fe^k\sqrt{2\pi\omega(k)}}e^{-\frac{(d_-)^2}{2}} \quad (2.27)$$

is non-decreasing, it follows that the density is admissible only if  $g(k) \geq 0 \ \forall k$ . Next, the condition that  $\lim_{k \rightarrow +\infty} d_+(k) = -\infty$  ensures that call prices converge to zero as strikes tends to infinity. To see this, note that we can equivalently write the solution to the price of a call option under Black-Scholes in terms of the complementary cumulative normal distribution function, which we will denote  $\Phi(\cdot)$  and satisfies  $\Phi(-x) = N(x)$ , as

$$C_{BS} = S(\Phi(-d_+) - e^k\Phi(-d_-)) = S(\Phi(-d_+) - e^k\Phi(-(d_+ - \sqrt{\omega(k)}))). \quad (2.28)$$

By the AM-GM inequality,

$$-(d_+ - \sqrt{\omega(k)}) = \frac{k}{\sqrt{\omega(k)}} + \frac{\sqrt{\omega(k)}}{2} \geq \sqrt{2k}. \quad (2.29)$$

We thus have that

$$e^k\Phi(-(d_+ - \sqrt{\omega(k)}) \leq e^k\Phi(\sqrt{2k}) \leq \frac{1}{2\sqrt{\pi k}} \rightarrow 0 \text{ as } k \rightarrow \infty. \quad (2.30)$$

Thus, to ensure that call prices do indeed tend to zero as  $K \rightarrow \infty \Leftrightarrow k \rightarrow \infty$ , it is only necessary that the term  $\Phi(-d_+) \rightarrow 0$  as  $d_+ \rightarrow \infty$ , which is equivalent to  $N(d_+) \rightarrow 0$  as

$d_+ \rightarrow -\infty$ , which is further equivalent to requiring that  $d_+ \rightarrow -\infty$  as  $k \rightarrow \infty$ . ■

## 3 Parameterizing the Implied Volatility Surface

### 3.1 Gatheral's and Jacquier's SVI and SSVI

#### 3.1.1 The SVI Model

One of the earlier attempts to directly parameterize implied volatility was Jim Gatheral's SVI model (see [Gatheral 2004] and [Gatheral and Jacquier 2013]). The model remains popular due to its favorable performance (driven mainly by its piecewise or expiry-independent nature; more on this below) and limiting behavior. That is, for any time  $t$  the total implied variance  $\omega(k, t) = \sigma_{BS}^2(k, t)t$  is linear in extreme strikes  $K$  (i.e. those that are far from the forward price  $F_t$  or as  $k \rightarrow \infty$  or  $k \rightarrow -\infty$ ). This is consistent with Lee's moment formula (see [Lee 2004]), which showed that in the absence of arbitrage, for any time  $t$  the extreme-strike tail of Black-Scholes implied variance skew (that is, the slope of the implied variance curve for any time  $t$  over some range of strikes far from the forward price  $F_t$ ) is bounded by  $\frac{2|k|}{t}$ , or equivalently that total implied variance  $\omega(k, t)$  is bounded by  $2|k|$ . In practice, the consistent behavior of the model with this property is important as it allows for reasonable confidence in modeling/extrapolation of off-market strikes that may likewise be far away from the forward level.

For a given maturity  $t$ , the SVI parameterization of total implied variance reads:

$$\omega(k) = a + b \left\{ \rho(k - m) + \sqrt{(k - m)^2 + \sigma^2} \right\}, \quad (3.1)$$

where  $a, m \in \mathbb{R}, b \geq 0, |\rho| < 1, \sigma > 0$ , and  $a + b\sigma\sqrt{1 - \rho^2}$  so that  $\omega(k) \geq 0 \forall k \in \mathbb{R}$ . Note that the strict inequalities on  $\rho$  and  $\sigma$  simply exclude trivial cases where the volatility smile is either strictly increasing or decreasing, or linear, respectively, although it would be perfectly acceptable to introduce the equality into these conditions.

#### 3.1.2 Absence of Arbitrage in the SVI Model

In Section 2.2.2, the idea of the absence of arbitrage on a volatility surface was introduced and conditions derived to ensure this property across the time (calendar spread) and spatial (butterfly spread) dimensions. The SVI parameterization introduced above in Equation (3.1) does not truly define a volatility *surface*, as seen by the lack of dependence of  $\omega$  on  $t$ . Equation (3.1) simply defines a slice of the volatility surface for a given maturity  $t$ , so a volatility surface

would only be the result of a collection of these slices for a number of different maturities  $t_i$ . This begets the main limitation of the SVI model, as deriving conditions to ensure the absence of arbitrage are either entirely too complicated, both analytically and computationally, or perhaps not available at all. For instance, in [**Gatheral and Jacquier 2013**], the condition ensuring the absence of calendar spread arbitrage is that the following quartic polynomial has no real root:

$$\alpha_4 k^4 + \alpha_3 k^3 + \alpha_2 k^2 + \alpha_1 k + \alpha_0 = 0, \quad (3.2)$$

where the expressions for the coefficients are too lengthy to make it reasonable to include herein<sup>3</sup>. Even notwithstanding this, there is further no known general conditions on the parameters which eliminates butterfly spread arbitrage.

### 3.1.3 The SSVI Model

In [**Gatheral and Jacquier 2013**], the SSVI, or "surface SVI" model is introduced as an expiry-dependent extension of the SVI model. For any time  $t \geq 0$ , we define at-the-money (ATM), or zero log moneyness ( $k = 0$ ), total implied variance as  $\theta_t = \sigma_{BS}^2(0, t)t = \omega(0, t)$ . Assuming  $\theta$  is at least of class  $C^1$  on  $\mathbb{R}_+^*$ ,  $\lim_{t \rightarrow 0} \theta_t = 0$ , and that  $\varphi$  is a smooth function from  $\mathbb{R}_+^*$  to  $\mathbb{R}_+^*$  such that  $\lim_{t \rightarrow 0}$  exists in  $\mathbb{R}$ , the SSVI surface of implied total variance is given by

$$\omega(k, \theta_t) = \frac{\theta_t}{2} \left\{ 1 + \rho \varphi(\theta_t)k + \sqrt{(\varphi(\theta_t)k + \rho)^2 + (1 - \rho^2)} \right\}, \quad (3.3)$$

with  $|\rho| < 1$  representing the correlation between the underlying price and its instantaneous volatility (typically negative), resulting in a symmetric smile around  $k = 0$  if and only if  $\rho = 0$ .

### 3.1.4 Absence of Arbitrage in the SSVI Model

Unlike the SVI model, general, sufficient conditions can be found such that the SSVI volatility surface given in Equation (3.3) is free of both calendar spread and butterfly arbitrage. These conditions are provided in the following two theorems. Detailed proofs were originally provided in [**Gatheral and Jacquier 2013**]. Those herein follow these closely, with some additional detail given in the hopes that the reader benefits (as did the author) from a degree of work-through and clarification of these more abstruse proofs.

---

<sup>3</sup>For the interested reader, they can be found within an R code at <http://faculty.baruch.cuny.edu/jgatheral>

**Theorem 3.1** (Theorem 4.1 in [Gatheral and Jacquier 2013]). *The SSVI surface (3.3) is free of calendar spread arbitrage if and only if:*

$$(i) \quad \frac{\partial \theta_t}{\partial t} \geq 0, \text{ for all } t \geq 0, \text{ and} \quad (3.4)$$

$$(ii) \quad 0 \leq \frac{\partial(\theta\varphi(\theta))}{\partial\theta} \leq \frac{1 + \sqrt{1 - \rho^2}}{\rho^2} \varphi(\theta). \quad (3.5)$$

*Proof.* From Lemma (2.1) and the chain rule, we have that

$$\frac{\partial \omega(k, \theta_t)}{\partial t} = \frac{\partial \omega(k, \theta_t)}{\partial \theta_t} \frac{\partial \theta_t}{\partial t}. \quad (3.6)$$

In the proof of Lemma (2.1) we also saw that  $C_{BS}$  is non-decreasing in its second argument and as a result  $\omega(k, \theta_t)$  must also be non-decreasing in its second argument. Condition (i) then follows immediately. We thus have only remaining to prove that the parameterization is in fact increasing in  $\theta_t$ . Letting  $\gamma = \frac{\partial(\theta\varphi(\theta))}{\partial\theta}/\varphi(\theta) = (1 + \frac{\theta \frac{\partial \varphi(\theta)}{\partial \theta}}{\varphi(\theta)})$  and  $x = k\varphi(\theta)$ , we can write

$$2 \frac{\partial \omega(k, \theta)}{\partial \theta} = \psi_0(x, \rho) + \gamma \psi_1(x, \rho), \quad (3.7)$$

with

$$\psi_0(x, \rho) = 1 + \frac{1 + \rho x}{\sqrt{x^2 + 2\rho x + 1}} \quad \text{and} \quad \psi_1(x, \rho) = x \left( \frac{x + \rho}{\sqrt{x^2 + 2\rho x + 1}} + \rho \right). \quad (3.8)$$

For  $|\rho| < 1$ ,  $\psi_0(x, \rho)$  is strictly positive for all  $x \in \mathbb{R}$ . Furthermore, when  $x \in \{0, -2\rho\}$ ,  $\psi_1(x, \rho) = 0$  and thus  $\frac{\partial \omega(k, \theta)}{\partial \theta} \geq 0$ . It can be shown that  $\psi_1(\cdot, \rho) > 0$  of  $x \in \mathcal{D}_\rho$  and  $\psi_1(\cdot, \rho) < 0$

if  $x \in \mathbb{R} \setminus (\mathcal{D}_\rho \cup \{0, -2\rho\})$ , where

$$\mathcal{D}_\rho = \begin{cases} (-\infty, 0) \cup (-2\rho, \infty), & \text{if } \rho < 0, \\ (-\infty, -2\rho) \cup (0, \infty), & \text{if } \rho > 0, \\ \mathbb{R} \setminus \{0\}, & \text{if } \rho = 0. \end{cases} \quad (3.9)$$

It follows that

$$\frac{\partial \omega(k, \theta)}{\partial \theta} \geq 0 \text{ iff } \begin{cases} \gamma \geq -\frac{\psi_0(x, \rho)}{\psi_1(x, \rho)}, & \text{for } x \in \mathcal{D}_\rho, \\ \gamma \leq -\frac{\psi_0(x, \rho)}{\psi_1(x, \rho)}, & \text{for } x \in \mathbb{R} \setminus (\mathcal{D}_\rho \cup \{0, -2\rho\}). \end{cases} \quad (3.10)$$

The tightest possible bounds will thus be given by  $\sup_{x \in \mathcal{D}_\rho} -\psi_0(x, \rho)/\psi_1(x, \rho)$  and  $\inf_{x \in \mathbb{R} \setminus (\mathcal{D}_\rho \cup \{0, -2\rho\})} -\psi_0(x, \rho)/\psi_1(x, \rho)$ . Visual inspection of this function, given below in Figure 5, makes the results to come a bit more obvious.

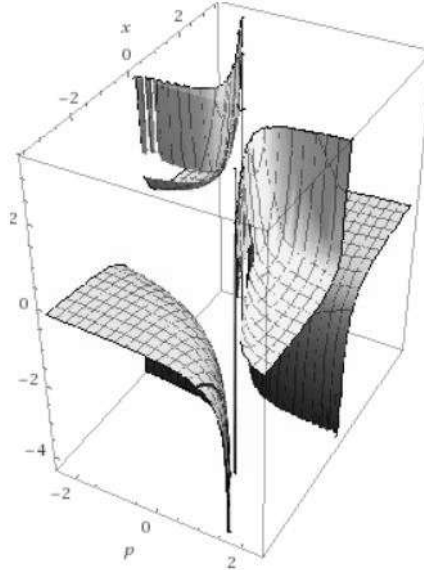


Figure 5: Graph of the function  $-\psi_0(x, \rho)/\psi_1(x, \rho)$

The supremum in  $\mathcal{D}_\rho$  is in fact  $\lim_{x \rightarrow \pm\infty} \frac{\psi_0(x, \rho)}{\psi_1(x, \rho)} = 0$ . Further, as

$$\frac{\partial}{\partial x} \left( -\frac{\psi_0(x, \rho)}{\psi_1(x, \rho)} \right) = \frac{(\rho + x) \left( \rho^2 x^2 + 2\rho x (\sqrt{x^2 + 2\rho x + 1} + 2) + 2\sqrt{x^2 + 2\rho x + 1} + x^2 + 2 \right)}{x^2 \sqrt{x^2 + 2\rho x + 1} \left( \rho \sqrt{x^2 + 2\rho x + 1} + \rho + x \right)^2}, \quad (3.11)$$

the infimum in  $\mathbb{R} \setminus (\mathcal{D}_\rho \cup \{0, -2\rho\})$  is obtained at  $x = -\rho$ , and

$$-\frac{\psi_0(-\rho, \rho)}{\psi_1(-\rho, \rho)} = \frac{1 + \sqrt{1 - \rho^2}}{\rho^2}. \quad (3.12)$$

■

**Theorem 3.2** (Theorem 4.2 in [Gatheral and Jacquier 2013]). *The SSVI surface (3.3) is free of butterfly arbitrage if for all  $\theta > 0$ :*

$$(i) \quad \theta\varphi(\theta)(1 + |\rho|) < 4, \text{ and} \quad (3.13)$$

$$(ii) \quad \theta\varphi(\theta)^2(1 + |\rho|) \leq 4. \quad (3.14)$$

*Proof.* Again letting  $x = k\varphi(\theta)$ , it can be found that Equation (2.24), given the SSVI parameterization of Equation (3.3), can be written as

$$g(x) = \frac{f(x)}{64(x^2 + 2x\rho + 1)^{3/2}}, \quad (3.15)$$

where

$$f(x) = a - b\varphi(\theta)^2\theta - \frac{c}{16}\varphi(\theta)^2\theta^2, \quad (3.16)$$

with  $a, b$ , and  $c$  all depending on  $x$ . Assuming that  $\theta\varphi(\theta)(1 + |\rho|) < 4$  and  $\theta\varphi(\theta)^2(1 + |\rho|) \leq 4$ , it can be shown that  $f(x) \geq 0 \ \forall x$  and thus  $g(x) \geq 0 \ \forall x$ . ■

## 3.2 Hendricks' and Martini's eSSVI

While the SSVI model offers important advantages over the SVI model related to the precise conditions available which preclude the possibility of arbitrage on the volatility surface, the parsimony of parameterizing the entire surface with just a few parameters tends to result in material reductions in performance as measured by the calibration error, or the ability of the model to reconstruct traded implied volatilities. In particular, incorporating a constant value for  $\rho$ , which recall represents the correlation between the underlying price and its instantaneous volatility, for all maturities is a restricting and in general empirically rejected assumption. Accordingly, in [Hendricks 2016] and [Hendricks and Martini 2019], the authors began to consider extending the SSVI model by increasing the degrees of freedom, specifically by generalizing the constant parameter  $\rho$  to a functional form dependent, much like  $\varphi$ , on the ATM implied total variance  $\theta$ . This parameterization, called extended surface SVI, or eSSVI, is given by

$$\omega(k, \theta_t) = \frac{\theta_t}{2} \left\{ 1 + \rho(\theta_t)\varphi(\theta_t)k + \sqrt{(\varphi(\theta_t)k + \rho(\theta_t))^2 + (1 - \rho(\theta_t)^2)} \right\}, \quad (3.17)$$

with  $\rho : \mathbb{R}_+^* \mapsto (-1, 1)$ .

### 3.2.1 Absence of Arbitrage in the eSSVI Model

In terms of sufficient conditions which ensure the absence of arbitrage on the eSSVI volatility surface, it is first important to note that the conditions concerning butterfly arbitrage have not changed from the SSVI model, as butterfly arbitrage is linked to the log moneyness  $k$ , and changing  $\rho$  to a function that depends not on  $k$  but on  $\theta_t$  does not therefore require any adjustment. In [Hendricks 2016], the conditions for the absence of calendar spread arbitrage are shown to be as in the following theorem.

**Theorem 3.3** *The eSSVI surface (3.17) is free of calendar spread arbitrage if for all  $\frac{\partial \theta_t}{\partial t} > 0$ ,  $|\delta + \rho\gamma| \leq \gamma$ , where  $\gamma = \frac{\partial(\theta\varphi(\theta))}{\partial\theta}/\varphi(\theta)$  and  $\delta = \theta\frac{\partial\rho(\theta)}{\partial\theta}$ , and either:*

$$(i) \quad \gamma \leq 1, \text{ or} \quad (3.18)$$

$$(ii) \quad |\delta + \rho\gamma| \leq \sqrt{2\gamma - 1}. \quad (3.19)$$

## 4 Model Calibrations

### 4.1 Risk-Neutral Calibration Methodology

The SSVI model (taken to also mean the various extensions considered here) can be calibrated to option prices, that is under the risk-neutral measure, by inverting the pricing problem and finding those model parameters which allow closest replication of market observed prices. Thus, taking market prices as a reference, the Black Scholes model can be used to calibrate the parameters of a given SSVI model by mapping the modeled implied volatilities to prices. To this end, an objective or cost function is constructed to achieve the best approximation to the data. As proposed in for instance [**Bakshi et. al. 1997**], we will use an average pricing error (*APE*), given by

$$APE = \min_{\tilde{\mathbf{v}}, \tilde{\theta}_t} \frac{1}{N} \sum_{i=1}^N \left| \frac{\text{market price}_i - \text{calculated price}_i}{\text{market price}_i} \right|, \quad (4.1)$$

where we have used  $\tilde{\mathbf{v}}$  to denote the parameters of the SSVI functions  $\varphi$  and  $\rho$ , and  $\tilde{\theta}_t$  to denote the ATM implied total variances, with the latter separated from the formers for reasons to be described shortly. However, we also will use the number of bid/ask violations as a measure of model performance, and so we incorporate this objective as a regularization term in our objective function. Thus, the final form of the objective function will be:

$$APE = \min_{\tilde{\mathbf{v}}, \tilde{\theta}_t} \frac{1}{N} \sum_{i=1}^N \left| \frac{\text{market price}_i - \text{calculated price}_i}{\text{market price}_i} \right| + \lambda \chi_i \sqrt{t_i}, \quad (4.2)$$

where  $\lambda$  is a penalty scalar (set to 1.5 throughout),  $\chi_i$  is an indicator function which takes the value of 1 if the modeled price of option  $i$  is in violation of its market bid/ask spread, and  $t_i$  is the tenor of option  $i$ . A significant issue remains due to the fact that Equation (4.2) can have many local minimizers, and thus the calibration may be non-unique and numerical schemes can be highly sensitive to the initial value choices. Further, Equation (4.2) seems to offer no prescription for dealing with arbitrage violations in the modeled or "calculated" prices, an issue of significant importance for an admissible parameterization. There are a few ways we can deal with these issues. With regards to the first, one obvious and perhaps most intuitive, though heuristic, method is to simply run the optimization multiple times with different initial parameter vectors, and choose the eventual calibration which most minimizes the cost function of Equation (4.2). For simplicity and to avoid the necessary technical discussion of

a more globalized approach, the multiple initial values approach was used throughout this study. Additionally, regarding the second issue of enforcing the no arbitrage conditions on the parameters, while some kind of regularization approach could likewise be used that applied a penalty factor to parameterizations which are found to violate the conditions, we do not want to consider the arbitrage conditions as a "trade-off" at all (that is, accepting an arbitrage-admitting model as long as the decrease in the minimization objective exceeds some hurdle), and simply increase Equation (4.2) by some arbitrarily high number (i.e. 1,000,000) whenever an arbitrage condition is violated.

Analyzing the SSVI parameterization of  $\omega(k, t)$ , one notices that the function collapses simply to  $\omega_t$  when  $k = 0$ , that is, when we are at exactly the forward ATM log moneyness level, the shape effects of the parameterization do not matter, and we are just estimating the at-the-money "backbone" of the implied variance surface. Thus, calibrations are all ran in a two-step procedure, with only the vector of ATM implied total variances,  $\theta_t$  first calibrated to the nearest forward ATM log moneyness strike available in the market for each tenor, with any reasonable but arbitrary initial parameterization for  $\varphi$  and  $\rho$  locked. Then, these calibrated  $\theta_t$  values are locked in for a second calibration to the entire dataset, now allowing the parameters of the  $\varphi$  and  $\rho$  functions to vary in search of the minimum of Equation (4.2). Before moving on, we need to discuss two remaining issues of importance, that is the data we will use to facilitate calibration, and explicit functional forms for  $\varphi$  and  $\rho$ .

## 4.2 Market Data and Input Assumptions

The dataset for the empirical analysis consists of the entire end-of-day option chain on the Standard and Poor's 500 index (S&P 500), obtained from the Chicago Board Options Exchange (CBOE) and known as the SPX Options Traditional product, for February 22nd, 2016. The contract has a European exercise style and is AM-settled on the 3rd Friday of every month. The average of the market bid and ask was used to proxy the market price, and following [Rosenberg 2002], the following filters were imposed upon the data:

- 1) Moneyness is constrained to  $-0.10 \leq (K/S_t - 1) \leq 0.10$ ,
- 2) Annualized implied volatility must be between 5% and 95%,
- 3) Remove options with premia below the lower bound, in particular  $\max(0, S_t - q_t S_t - K e^{-r_t(T-t)})$  for call options and  $\max(0, K e^{-r_t(T-t)} + q_t S_t - S_t)$  for put options,
- 4) Verify that call prices are a decreasing function of strike and that put options are an increasing function of strike.

In addition to these constraints, we also require that bid prices are greater than \$0.05, which tends to be just a dummy minimum quote for deep out-of-the-money options and therefore carries no informational value. Additionally, the underlying spot index price was obtained from Bloomberg. The risk-free yield curve was taken to be the Overnight Indexed Swap (OIS) curve

on the valuation date, and was bootstrapped using a simultaneous calibration of LIBOR deposit rates (short-term), Eurodollar futures contracts (medium-term), LIBOR swaps (long-term), and LIBOR-OIS basis swaps (all-term), all obtained from Bloomberg. A simultaneous calibration of the yield curve rather than a traditional bootstrapping procedure is needed when assuming OIS discounting since the LIBOR swap rates themselves become functions of an implied OIS rate and therefore there is no unique solution for both observed LIBOR and OIS rates. However, a final adjustment is made to these calibrated rates before using them as an input in the pricing model. Although traditional option pricing theory assumes that market makers can replicate options by borrowing and lending at the risk-free rate (here the calibrated OIS rates), in practice this is not true and there tends to be a "funding spread," or a difference between what market makers can actually borrow at and the risk-free rate. Although this funding spread is not directly observable, we can extract it from option prices, along with the implied dividend yield, another important input assumption which we have not mentioned yet, using the put-call parity relation for European option prices,

$$Se^{-q_t t} + P_K = C_K + Ke^{-(r_t + \gamma_t)t}, \quad (4.3)$$

where  $q_t$  is the continuous dividend yield for tenor  $t$ ,  $r_t$  is the risk-free, or OIS rate for tenor  $t$ , and  $\gamma_t$  is the funding spread for tenor  $t$ . This relation holds for all  $K$ , and can be rearranged as

$$\begin{aligned} K &= Se^{(r_t + \gamma_t - q_t)t} + e^{(r_t + \gamma_t)t}(P_K - C_K) \\ &= F + e^{(r_t + \gamma_t)t}(P_K - C_K), \end{aligned} \quad (4.4)$$

with  $F$  the forward price as given in Equation (2.6) or Equation (2.8), now just incorporating the additional funding spread  $\gamma_t$  over  $r_t$ . For each maturity  $t$  in the option chain, we can thus extract the dividend yield  $q_t$  and funding spread  $\gamma_t$  implied in option prices by a linear regression of strikes  $K$  on a vector of ones and the difference between put and call prices. The resulting coefficients of this regression will be the forward price,  $F$ , and a "growth factor" of  $e^{(r_t + \gamma_t)t}$ . Using the spot price  $S$  and the OIS rate  $r_t$  from the rate curve calibration procedure, values for  $q_t$  and  $\gamma_t$  can be backed out from these regression coefficients.

### 4.3 Choice of Functional Forms for $\varphi$ and $\rho$

Thus far, we have only considered the  $\varphi$  and  $\rho$  functions generally, defining them only up to their dependence on  $\theta_t$ . While a number of representations for  $\varphi$  have been considered in the

related literature, a simple power law of the form

$$\varphi(\theta_t) = \eta\theta_t^{-\lambda}, \quad (4.5)$$

can be found to work well both in terms of its modeling performance and analytical tractability. We will assume only this form for the  $\varphi$  function for the rest of the paper, and the implied assertion that alternative forms for this function may not offer meaningful improvements to the model will become clear below.

As shown by Equation (3.3), the SSVI model assumes a constant value for  $\rho$  and is thus only a functional form in the most trivial sense. For eSSVI, of which the main extension/contribution is the generalization of the constant  $\rho$  to a more meaningful functional representation, the form

$$\rho = a \cdot \exp(-b \cdot \theta_t) + c \quad (4.6)$$

was proposed and studied in [Hendricks 2016] and [Hendricks and Martini 2019]. We will assume this form for  $\rho$  moving forward whenever we speak of and utilize the eSSVI model.

## 4.4 Calibration Results for SSVI and eSSVI Models

### 4.4.1 SSVI Explicit No Arbitrage Conditions

We begin by calibrating the SSVI model to the real market options surface on February 22nd, 2016 data using the minimization objective discussed above in Section 4.1. Using Theorems 3.1 and 3.2, we can derive the explicit conditions for no arbitrage given  $\varphi = \eta\theta_t^{-\lambda}$  and  $\rho = \rho$ . In addition to requiring  $\eta > 0$  so that  $\varphi$  is positive, the condition (ii) of Theorem 3.1 tells us that we require:

$$0 \leq \frac{\partial(\theta\varphi(\theta))}{\partial\theta}/\varphi(\theta) = 1 - \lambda \leq \frac{1 + \sqrt{1 - \rho^2}}{\rho^2} \quad (4.7)$$

For any  $\rho \in (-1, 1)$ ,  $\frac{1 + \sqrt{1 - \rho^2}}{\rho^2} > 1$ , and thus in addition to the requirement that condition (i) from Theorem 3.1, or  $\frac{\partial\theta_t}{\partial t} \geq 0$ ,  $\forall t \geq 0$ , is satisfied, the calendar spread arbitrage conditions are satisfied as long as

$$\lambda \in [0, 1]. \quad (4.8)$$

For the butterfly arbitrage conditions of Theorem 3.2, we require:

$$\begin{cases} \theta_t \varphi(\theta_t) = \eta \theta_t^{1-\lambda} < \frac{4}{(1+|\rho|)} \iff \eta < \frac{4\theta_t^{\lambda-1}}{(1+|\rho|)} \\ \theta_t \varphi(\theta_t)^2 = \eta^2 \theta_t^{1-2\lambda} \leq \frac{4}{(1+|\rho|)} \iff \eta \leq \frac{2\theta_t^{\lambda-1/2}}{\sqrt{(1+|\rho|)}}. \end{cases} \quad (4.9)$$

First, since  $\lim_{\theta \rightarrow 0} \theta_t \varphi(\theta_t)^2 = \eta^2 \theta_t^{1-2\lambda} \rightarrow \infty$  when  $\lambda \in (1/2, 1]$ , we need to tighten the condition of Equation (4.8) to require that:

$$\lambda \in [0, 1/2]. \quad (4.10)$$

Additionally, since both  $\theta_t \varphi(\theta_t)$  and  $\theta_t \varphi(\theta_t)^2$  are increasing in  $\theta_t$ , the conditions will not hold for large enough  $\theta_t$  and fixed  $\eta$ . Following the argument of [**Hendricks 2016**], who notes that this is not an overly problematic result due to the finite option tenors available in the market<sup>4</sup>, we can replace  $\theta_t$  with its maximum value  $\theta_T$  and require that:

$$0 < \eta < \min\left(\frac{4\theta_T^{\lambda-1}}{(1+|\rho|)}, \frac{2\theta_T^{\lambda-1/2}}{\sqrt{(1+|\rho|)}}\right). \quad (4.11)$$

#### 4.4.2 SSVI Calibration Results

Utilizing the calibration methodology described in Section 4.1, the market data and input assumptions described in Section 4.2, and the explicit no-arbitrage conditions detailed above in Section 4.4.1, the SSVI model was calibrated to the market option surface on February 22nd, 2016. Figures 6 and 7 below show the modeled implied volatility against the implied volatility of the market bid and ask quotes for the various maturities that were available in the market. Subsequently, Figure 8 shows the percentage of quotes at each maturity in which the model was unable to produce a quote which lied within the bid/ask spread of the market.

---

<sup>4</sup>Even for the SPX contract, which is arguably the most liquid equity-based exchange traded option contract in the world, a periodically issued three-year LEAP (long-term equity appreciation) contract is the longest available maturity.

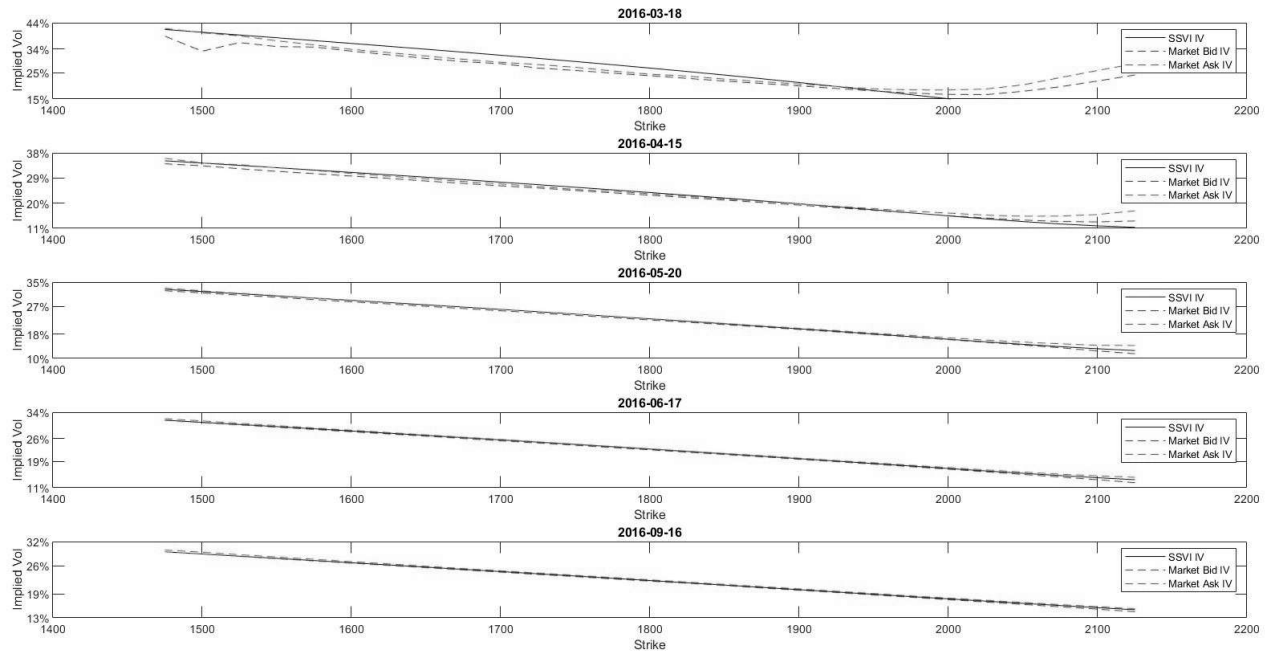


Figure 6: February 22nd, 2016 SSVI Implied Vol Fit Set 1

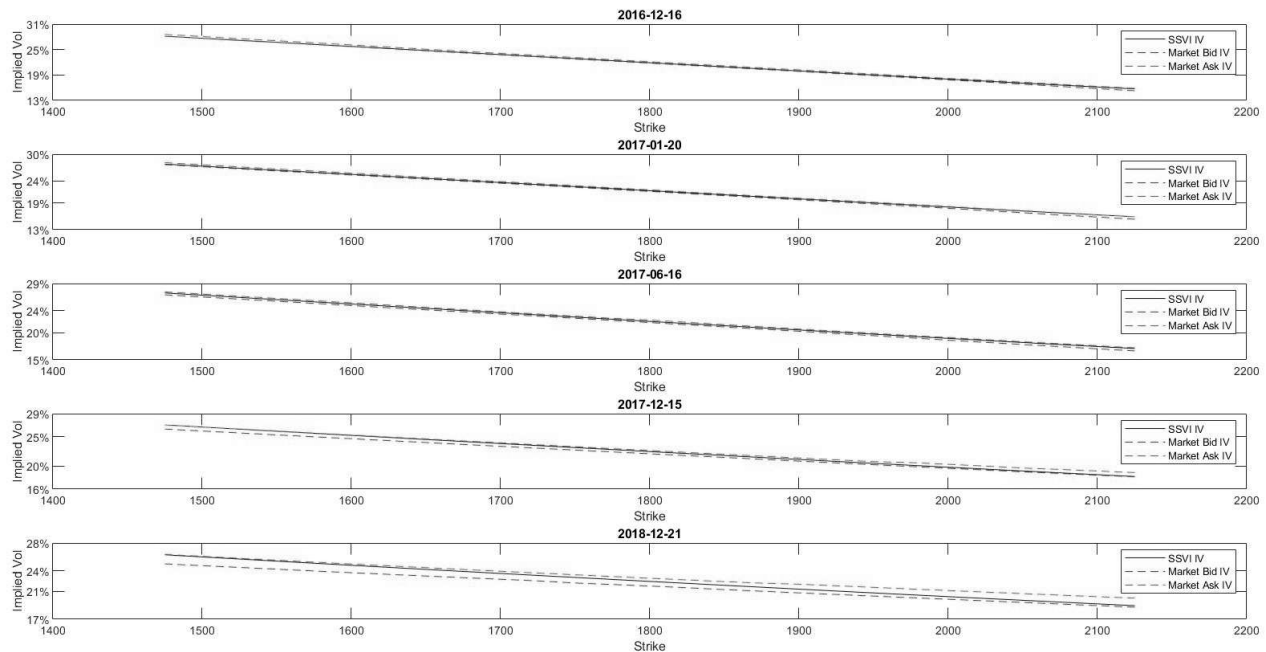


Figure 7: February 22nd, 2016 SSVI Implied Vol Fit Set 2

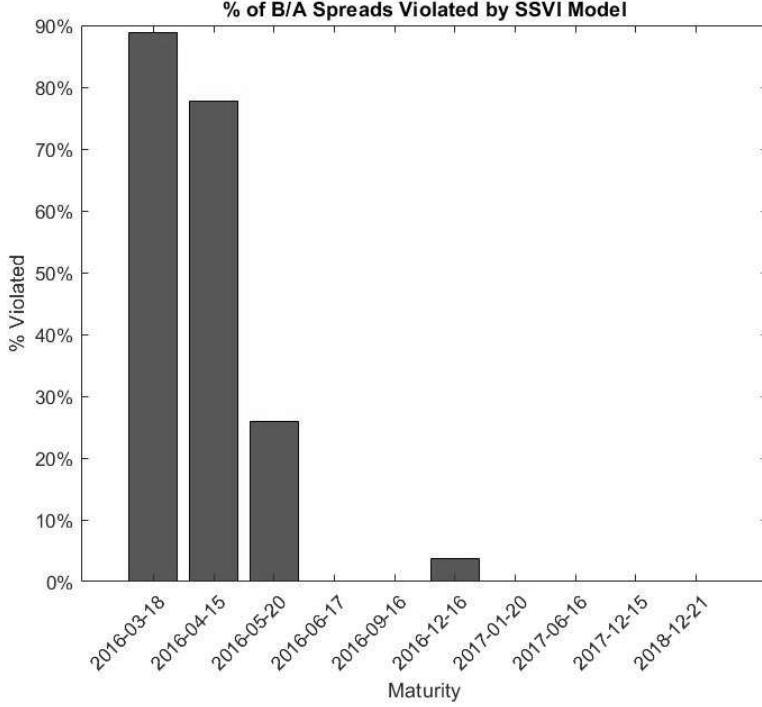


Figure 8: February 22nd, 2016 SSVI Implied Vol Fit Bid/Ask Spread Violations

#### 4.4.3 eSSVI Explicit No Arbitrage Conditions

We now move on to calibrating the eSSVI model to the real market options surface on February 22nd, 2016. Using Theorem 3.3, we can derive the explicit conditions for no arbitrage given  $\varphi = \eta\theta_t^{-\lambda}$  and  $\rho = a \cdot \exp(-b \cdot \theta_t) + c$ . First, however, recall from Section 3.2.1 that the butterfly arbitrage conditions do not change when moving from the SSVI to the eSSVI model. However, given the way we decided to write Equation (4.11) in terms of the maximum ATM total implied variance,  $\theta_T$ , a slight modification is needed given that  $\rho$  is now not a constant and thus the fractions on the right hand side of Equation (4.11) are not guaranteed to be increasing in  $\theta$ . So, again requiring  $\eta > 0$  so that  $\varphi$  is positive, we now require:

$$0 < \eta < \min_{0 \leq \theta_t \leq \theta_T} \left\{ \min \left( \frac{4\theta_t^{\lambda-1}}{(1 + |\rho(\theta_t)|)}, \frac{2\theta_t^{\lambda-1/2}}{\sqrt{(1 + |\rho(\theta_t)|)}} \right) \right\}. \quad (4.12)$$

Theorem 3.3 also gives the conditions for no calendar spread arbitrage, in addition to again requiring  $\frac{\partial \theta}{\partial t} \geq 0$ , as:

$$\begin{cases} |c - a/(1 - \lambda) \cdot \exp(\lambda - 2)| \leq 1, \\ |a + c| \leq 1, \\ |c| \leq 1. \end{cases} \quad (4.13)$$

*Proof.* First, we find that

$$\gamma = \frac{\partial(\theta\varphi(\theta))}{\partial\theta}/\varphi(\theta) = \frac{\eta\theta^{-\lambda}(1 - \lambda)}{\eta\theta^{-\lambda}} = (1 - \lambda) \quad (4.14)$$

Condition (i) of Theorem 3.3 is thus always satisfied as  $\lambda \in [0, 1/2]$ , and we are only left to require that

$$|\delta + \rho\gamma| \leq 1 \Leftrightarrow |\theta \frac{\partial\rho(\theta)}{\partial\theta} + \rho(\theta)(1 - \lambda)| \leq (1 - \lambda) \quad (4.15)$$

Due the positivity of  $(1 - \lambda)$  and evaluating the derivative term, we can write this as

$$|c + ae^{-b\theta} \frac{1 - \lambda - b\theta}{1 - \lambda}| \leq 1 \quad (4.16)$$

The left hand side obtains extremum at  $\theta = \frac{2-\lambda}{b}$ , and thus we consider this case along with  $\theta = 0$  and  $\lim_{\theta \rightarrow \infty}$  (recall  $\theta$  is non-negative and thus the case  $\lim_{\theta \rightarrow -\infty}$  not applicable). Evaluating the left hand side of Equation (4.16) at these values of  $\theta$  yields the conditions in Equation (4.13). ■

#### 4.4.4 eSSVI Calibration Results

Utilizing again the calibration methodology described in Section 4.1, the market data and input assumptions described in Section 4.2, and the explicit no-arbitrage conditions detailed above in Section 4.4.3, the eSSVI model was calibrated to the market option surface on February 22nd, 2016. Figures 9 and 10 below show the modeled implied volatility against the implied volatility of the market bid and ask quotes for the various maturities that were available in the market. Subsequently, Figure 11 shows the percentage of quotes at each maturity in which the model was unable to produce a quote which lied within the bid/ask spread of the market. It is clear

that the eSSVI model offers an improved fit to the real market options surface when compared to the SSVI model, as expected by the extra degrees of freedom in generalizing the  $\rho$  parameter.

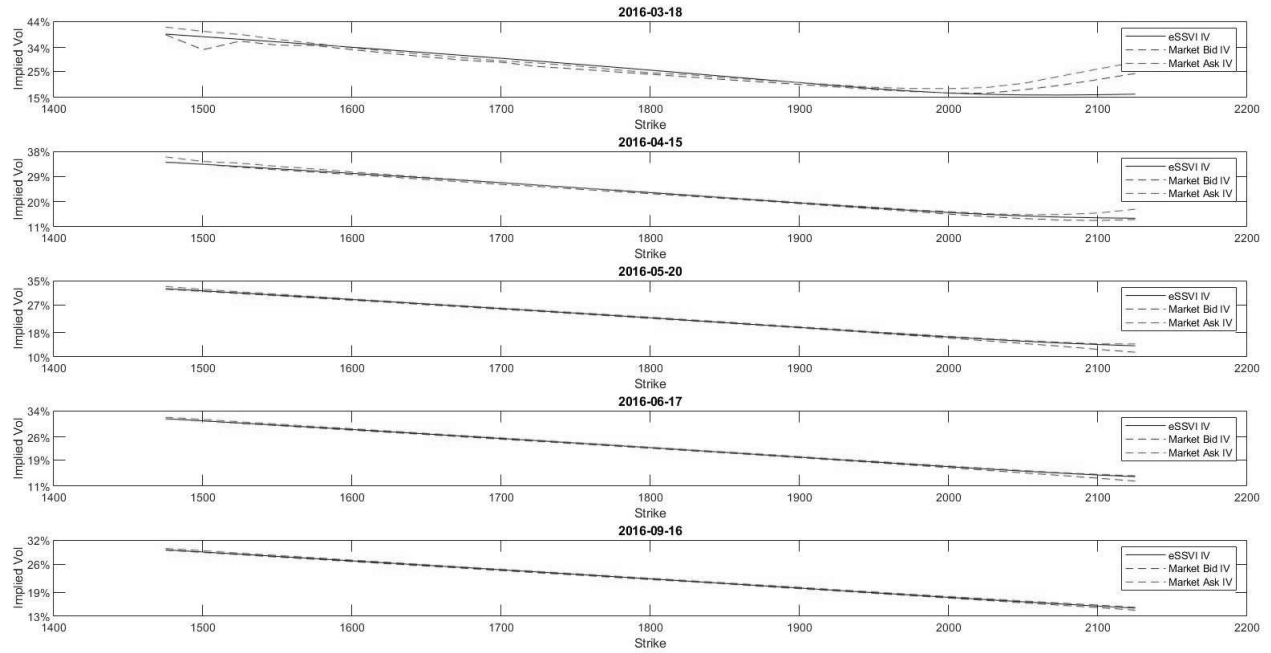


Figure 9: February 22nd, 2016 eSSVI Implied Vol Fit Set 1

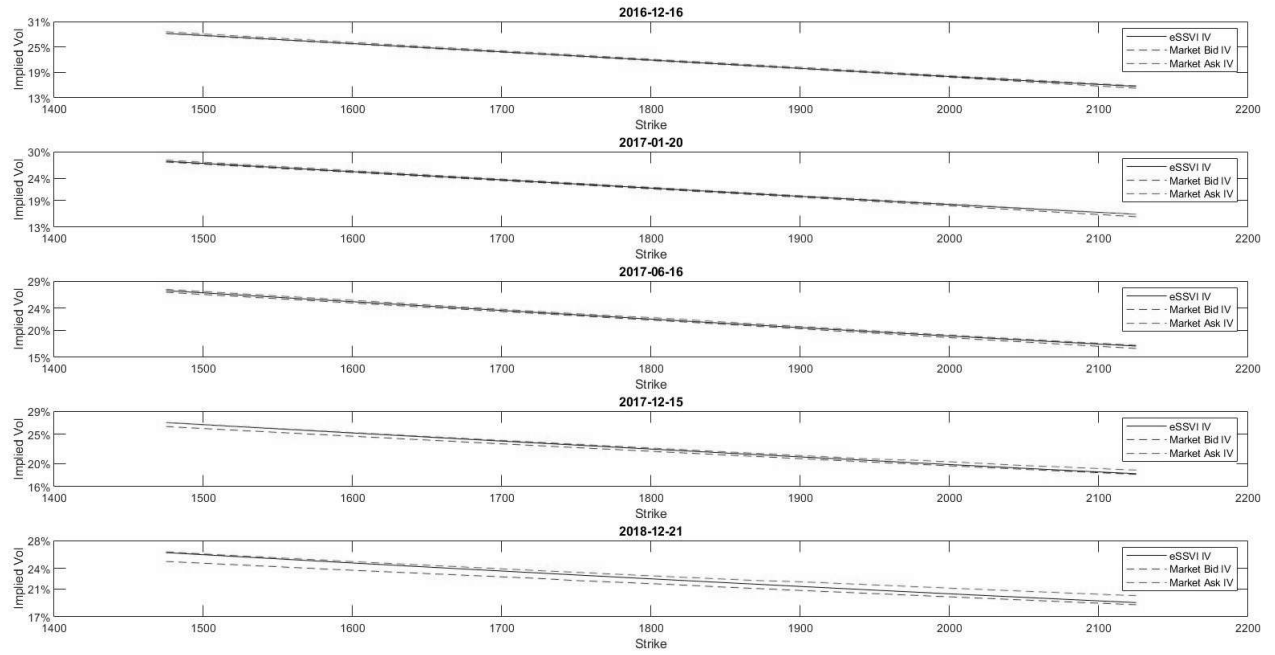


Figure 10: February 22nd, 2016 eSSVI Implied Vol Fit Set 1

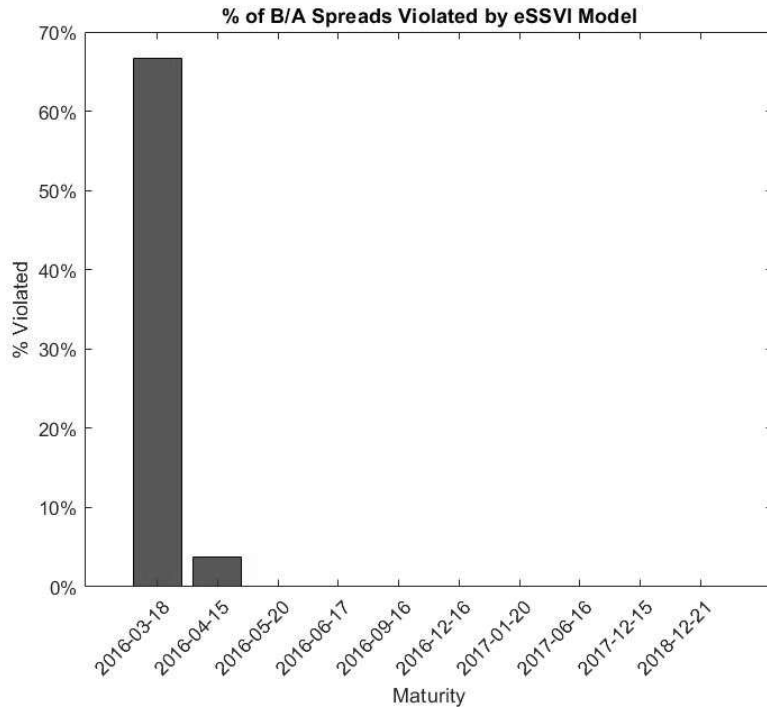


Figure 11: February 22nd, 2016 eSSVI Implied Vol Fit Bid/Ask Spread Violations

## 5 Generalizing the Functional Form for Correlation

### 5.1 Motivation

As shown above, although the improvement in model fit offered by the eSSVI's generalization of the  $\rho$  parameter is material, there still appears to be plenty of room for improvement on the short end of the implied volatility surface, as even for the eSSVI model we are violating nearly 70% of the market bid/ask spreads for the nearest option maturity.<sup>5</sup> The question is, what should the functional forms for  $\varphi$  and  $\rho$  look like if not the forms already considered? Given that the model fit of the eSSVI parameterization was not entirely unsatisfactory and only a bit wanting in certain areas, we can motivate the research of alternative functional forms in the following way. The eSSVI model will be fit piecewise to each option maturity, and this family of eSSVI models will be investigated for clues about which direction to take in search of more applicable parameterizations. Figures 12 - 14 below show the familiar illustrations of the implied volatility fit by maturity of the calibrated piecewise eSSVI model, where we see that given the flexibility to consider dedicated models for each tenor, the fit of the model is further improved, and with a near 70% decrease in the number of nearest maturity violations compared to the "complete" model.

---

<sup>5</sup>While this would be perhaps excusable if "nearest" maturity meant an exceedingly short period, i.e. 1 or 2 days, we note that for our valuation date of February 22nd, 2016, the next monthly expiry of March 18th, 2016 is approximately an entire month away.

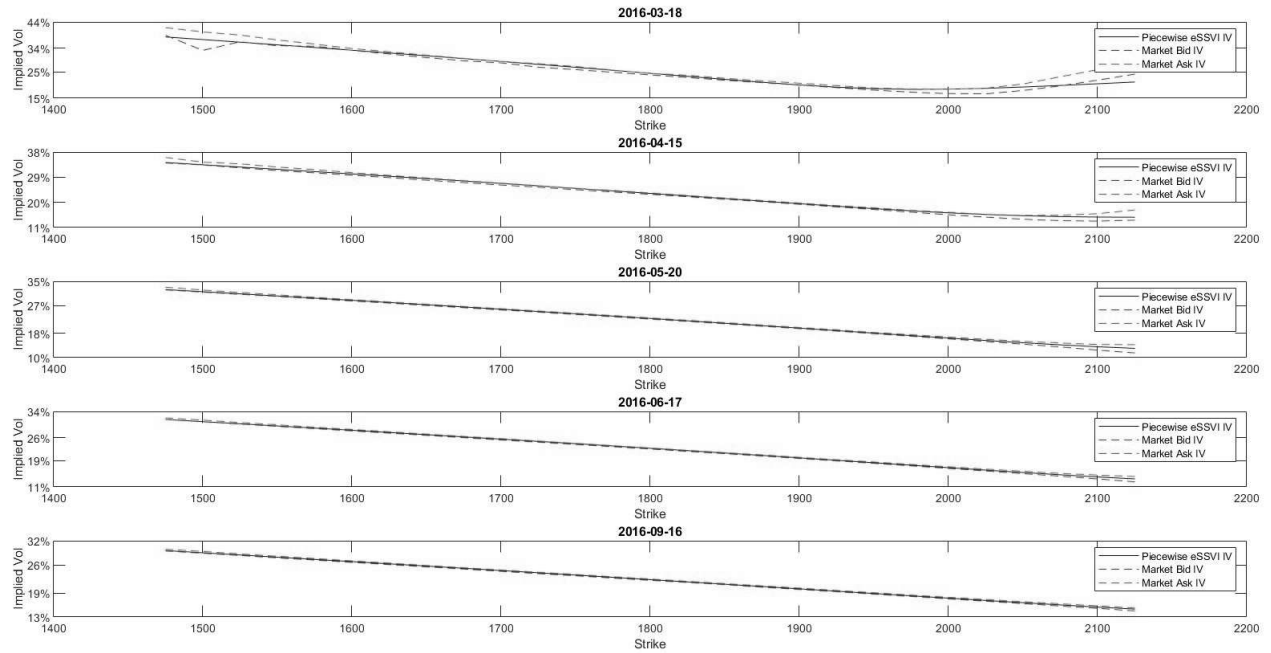


Figure 12: February 22nd, 2016 Piecewise eSSVI Implied Vol Fit Set 1

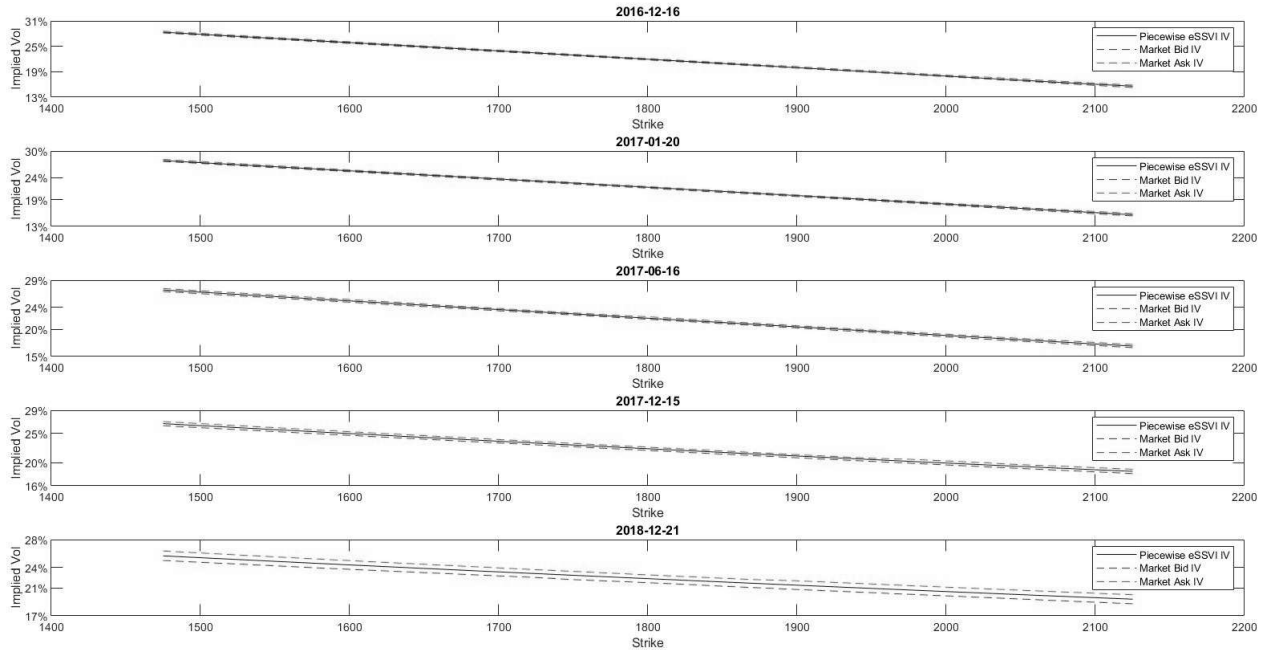


Figure 13: February 22nd, 2016 Piecewise eSSVI Implied Vol Fit Set 2

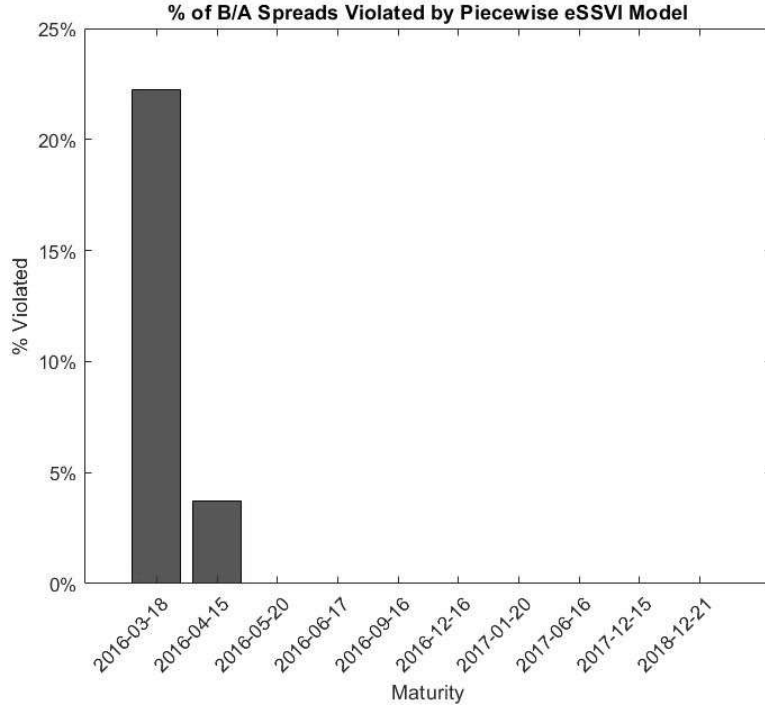


Figure 14: February 22nd, 2016 Piecewise eSSVI Implied Vol Fit Bid/Ask Spread Violations

To answer the question of what the functions look like which produce the above results, we evaluate the  $\varphi$  and  $\rho$  functions for each model of the piecewise family of eSSVI models at their respective  $\theta_t$  values, and apply some kind of interpolation scheme to fill in the points between these discrete points on the domain. To this end, a simple average of a cubic spline and an akima spline is applied, in order to produce smooth functions but with some tempering of the extreme oscillations that can be produced purely by a cubic spline. The results of this procedure are shown below in Figures 15 and 16.

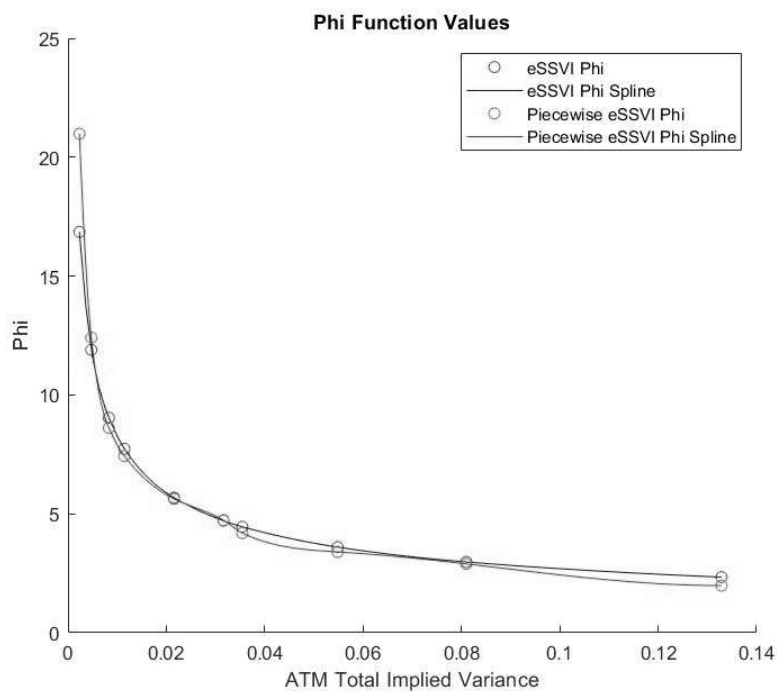


Figure 15: Total and Piecewise eSSVI Phi Functions

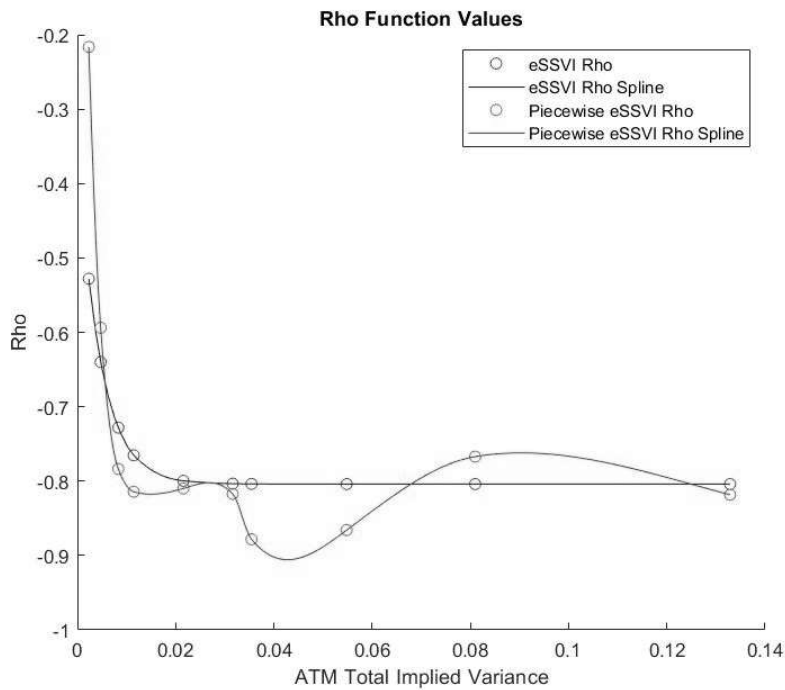


Figure 16: Total and Piecewise eSSVI Rho Functions

From Figure 15, we see that the basic power law representation for  $\varphi$ , that is  $\eta\theta_t^{-\lambda}$ , appears to apply reasonably well whether we are fitting the entire surface with a single parameterization or with a dedicated piecewise family of models. However, Figure 16 signals that there may be much incremental performance available in considering alternative forms for the functional form of  $\rho$ , as differences here are apparent. This is admittedly a naive method of inference, as it could be that the  $\varphi$  function has a materially higher attributable effect on the volatility surface even for minor perturbations and the  $\rho$  function is simply reacting in a compensatory way. However, given the intuition behind the influence of  $\rho$  on the surface, which recall importantly affects the symmetry of the smile across moneyness, we are also to some degree validated by additional visual evidence such as Figures 1 and 2 which show that this symmetry does in fact vary by maturity. An important question remains as to whether or not the piecewise calibrated model is holistically free of arbitrage. The answer is, unfortunately, no. Figure 17 below shows an example of a violation of the calendar spread arbitrage condition, which recall effectively states that no two implied variance curves in  $\theta_t$  may cross for any  $k$ .

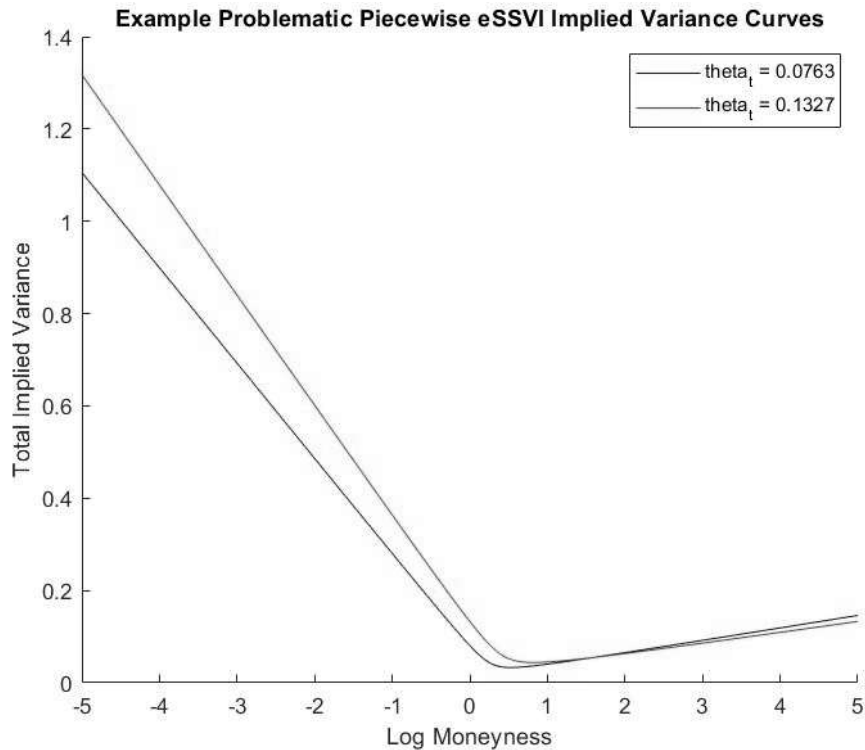


Figure 17: Example Arbitrage Violation on the Piecewise eSSVI Surface

Note that these are not the only values for  $\theta_t$  with which this is an issue and are specifically chosen only for illustrative purposes. Still, given the naive (that is, without any constraints to remove arbitrage) method with which we interpolated this piecewise surface, we will still

move forward with exploring alternative functional forms for  $\rho$  that are able to better capture the behavior illustrated in Figure 16, and allow the derived arbitrage constraints to tell us if such a model can provide the expected performance improvement in an admissible way.

## 5.2 The RxSSVI Model

The results above motivate the search for a function that can approximate the form shown in Figure 16, that is a smooth function with flexibility particularly towards the front end of its domain, but that has an overall exponentially decaying and horizontally asymptotic behavior in the large limit. This may motivate as a natural starting point the Fourier-Laguerre series,

$$\rho_k(\theta_t) = c + e^{-b\theta_t} \sum_{k=0}^N a_k L_k(\beta\theta_t), \quad (5.1)$$

with  $L_i(x)$  the Laguerre polynomials of degree  $k$ , defined compactly by the Rodrigues formula,

$$L_k(x) = \frac{e^x}{k!} \frac{d^k}{dx^k} (x^k e^{-x}), \quad (5.2)$$

and recursively for  $k \geq 2$

$$L_k(x) = \frac{1}{k} [(2k - 1 - x) \cdot L_{k-1}(x) - (k - 1) \cdot L_{k-2}(x)]. \quad (5.3)$$

This leads, for example, to the following forms for  $\rho$  up to the third order. Notice that for order  $k = 0$ , we simply have the eSSVI model, that is eSSVI is a special case of Equation (5.1) when  $k = 0$ .

$$\rho_0(\theta_t) = c + e^{-b\theta_t} \cdot a_0, \quad (5.4)$$

$$\rho_1(\theta_t) = c + e^{-b\theta_t} \cdot a_0 + e^{-b\theta_t} \cdot a_1 b\theta_t, \quad (5.5)$$

$$\rho_2(\theta_t) = c + e^{-b\theta_t} \cdot a_0 + e^{-b\theta_t} \cdot a_1 b\theta_t + e^{-b\theta_t} \cdot a_2 (b\theta_t)^2, \quad (5.6)$$

$$\rho_3(\theta_t) = c + e^{-b\theta_t} \cdot a_0 + e^{-b\theta_t} \cdot a_1 b\theta_t + e^{-b\theta_t} \cdot a_2 (b\theta_t)^2 + e^{-b\theta_t} \cdot a_3 (b\theta_t)^3. \quad (5.7)$$

However, one finds that the behavior in Figure 16 is not easily approximated when restricted to a single decay factor,  $e^{-bx}$ . The reader may recognize Equation (5.5) as the Nelson-Siegel

model [Nelson and Siegel 1987] of the yield curve, and we can therefore find inspiration for a more flexible set of models from the extensions of this model, à la Svensson [Svensson 1994]. We thus have instead, which we will call the RxSSVI Model, the following parameterization for  $\rho : \mathbb{R}_+^* \mapsto (-1, 1)$ :

$$\rho_k(\theta_t) = c + e^{-b_0\theta_t}a_0 + \sum_{k=1}^N e^{-b_{k-1}\theta_t}a_kb_{k-1}\theta_t, \quad (5.8)$$

and therefore the functional forms for  $\rho$  up to the third order are now (notice that we still have the eSSVI model when  $k = 0$ ):

$$\rho_0(\theta_t) = c + e^{-b_0\theta_t} \cdot a_0, \quad (5.9)$$

$$\rho_1(\theta_t) = c + e^{-b_0\theta_t} \cdot a_0 + e^{-b_0\theta_t} \cdot a_1 b_0 \theta_t, \quad (5.10)$$

$$\rho_2(\theta_t) = c + e^{-b_0\theta_t} \cdot a_0 + e^{-b_0\theta_t} \cdot a_1 b_0 \theta_t + e^{-b_1\theta_t} \cdot a_2 b_1 \theta_t, \quad (5.11)$$

$$\rho_3(\theta_t) = c + e^{-b_0\theta_t} \cdot a_0 + e^{-b_0\theta_t} \cdot a_1 b_0 \theta_t + e^{-b_1\theta_t} \cdot a_2 b_1 \theta_t + e^{-b_2\theta_t} \cdot a_3 b_2 \theta_t. \quad (5.12)$$

### 5.3 No-Arbitrage Conditions

Unfortunately, even extending the model with one additional factor as in Equation (5.10) leads to a significant increase in the complexity of the no-arbitrage (calendar spread, specifically) conditions. For example, by Theorem (3.3) (and still assuming  $\varphi(\theta_t) = \eta\theta_t^{-\lambda} \implies \gamma = 1 - \lambda$ ), for no-arbitrage we require that

$$\left| e^{-b_0} \left[ \frac{b_0\theta_t(a_1(1 - b_0\theta_t) - a_0)}{1 - \lambda} + a_0 + a_1 b_0 \theta_t \right] + c \right| \leq 1. \quad (5.13)$$

The left-hand-side has extrema at

$$\theta_t = \pm \left\{ \frac{\sqrt{a_0^2 - 2a_0a_1\lambda + a_1^2(\lambda^2 - 4\lambda + 8)} + a_0 + a_1\lambda - 4a_1}{2b_0a_1} \right\}, \quad (5.14)$$

and evaluating Equation (5.13) at this point is no simple task, let alone what it implies for the higher order models. Still, the no arbitrage conditions and the relevant derivatives, extrema, etc. can be handled without too much difficulty numerically, and therefore the inability to put the conditions to paper does not impede exploration of the model. Also, note that for all orders of the model, the limiting behavior of the condition required from Theorem 3.3 (i.e. those analogous to Equation (5.13)) as  $\theta_t \rightarrow 0$  and  $\theta_t \rightarrow \infty$  still requires for all models, as in the eSSVI model,

$$\begin{cases} |a + c| \leq 1, \\ |c| \leq 1. \end{cases} \quad (5.15)$$

## 5.4 Calibration Results for Rx Models

Utilizing again the calibration methodology described in Section 4.1, the market data and input assumptions described in Section 4.2, and no-arbitrage conditions found numerically as described above, the RxSSVI model was calibrated to the market option surface on February 22nd, 2016 for order  $k = 1, 2, 3$  (recall order  $k = 0$  is just the eSSVI model). Table 1 and Figure 18 below show a summary of the calibrated parameters for all models, including the SSVI and eSSVI models already calibrated, and a comparison of the percentage of quotes at each maturity in which the models were unable to produce prices which lied within the bid/ask spread of the market, respectively.

Table 1: Model Calibrations Summary

<b>Model</b>	$\eta$	$\lambda$	$c$	$\alpha_0$	$\alpha_1$	$\alpha_2$	$\alpha_3$	$\beta_0$	$\beta_1$	$\beta_2$	<b>APE</b>
SSVI	0.9122	0.4706	-0.8114								0.1256
eSSVI	0.8721	0.4883	-0.8040	0.4547				215.0487			0.0399
R1	0.8822	0.4865	-0.8008	0.4645	0.0063			222.8563			0.0398
R2	0.8866	0.4871	-0.7993	0.5494	-0.3299	0.3100		242.2611	214.9029		0.0379
R3	0.8828	0.4918	-0.7860	0.6011	-0.2769	0.3348	-0.0676	261.6977	203.2310	147.2328	0.0363

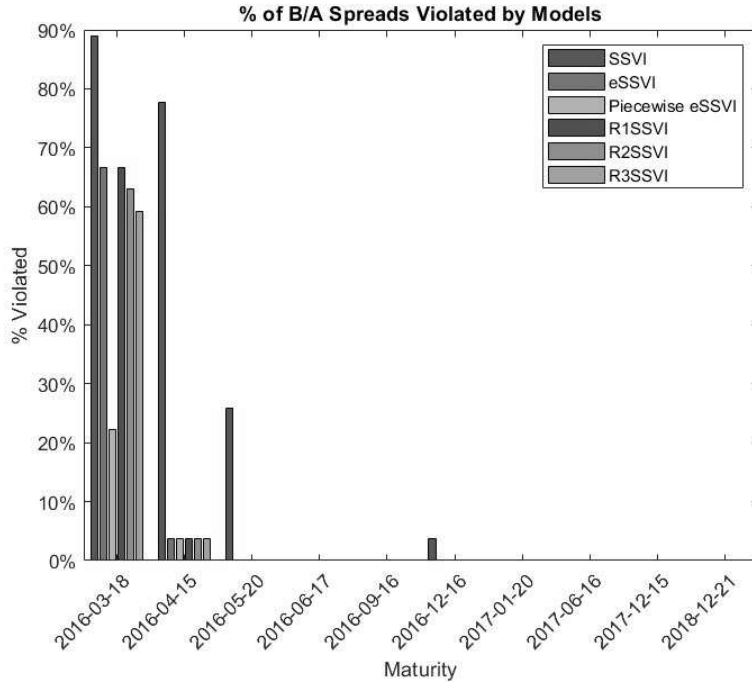


Figure 18: February 22nd, 2016 Implied Vol Fit Bid/Ask Spread Violations - All Models

The subsequent subsections show results for each Rx model, which include comparisons of the  $\rho$  function produced by each calibration. As shown, the arbitrage constraints prove to be too restrictive to allow a meaningful replication of the piecewise function. Figure 18 above already alluded to this inefficacy, as the reduction in the number of bid/ask violations for the nearest maturity was rather meager for each increase in order for the model. As a means to offer some visual proof that this in fact must be due to no-arbitrage restrictions and not a mistake in the functional form chosen for  $\rho$ , Figure 31 gives a direct fit for the third order model (that is, a direct least squares is run on the piecewise function itself, bypassing any option pricing). As shown, the multiple inflection points afforded by the functional form for a third order model should be able to closely match the knot points of the piecewise fit function. A calibration run of the third order model with this direct fit function for  $\rho$ , however, is immediately rejected for violating arbitrage constraints.

### 5.4.1 R1 Model

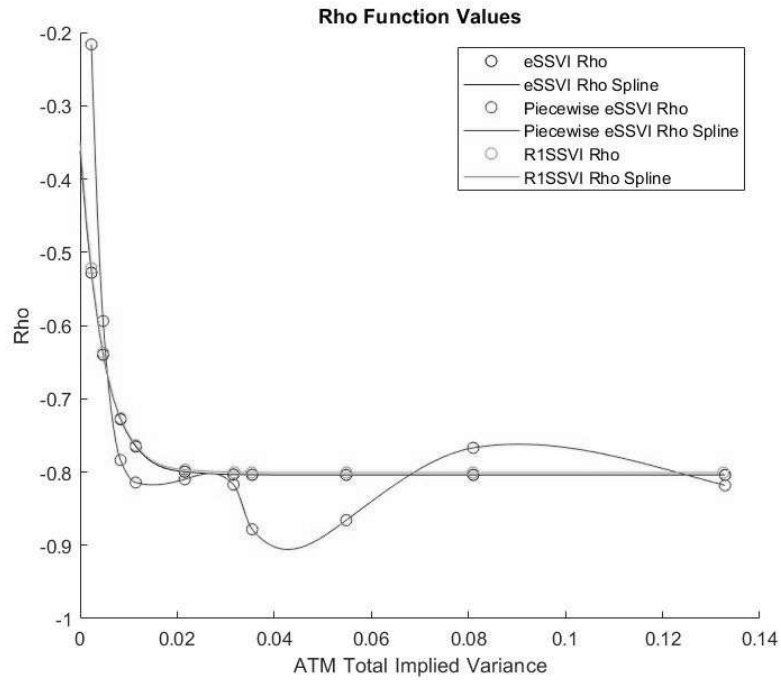


Figure 19: Rho Function Comparisons

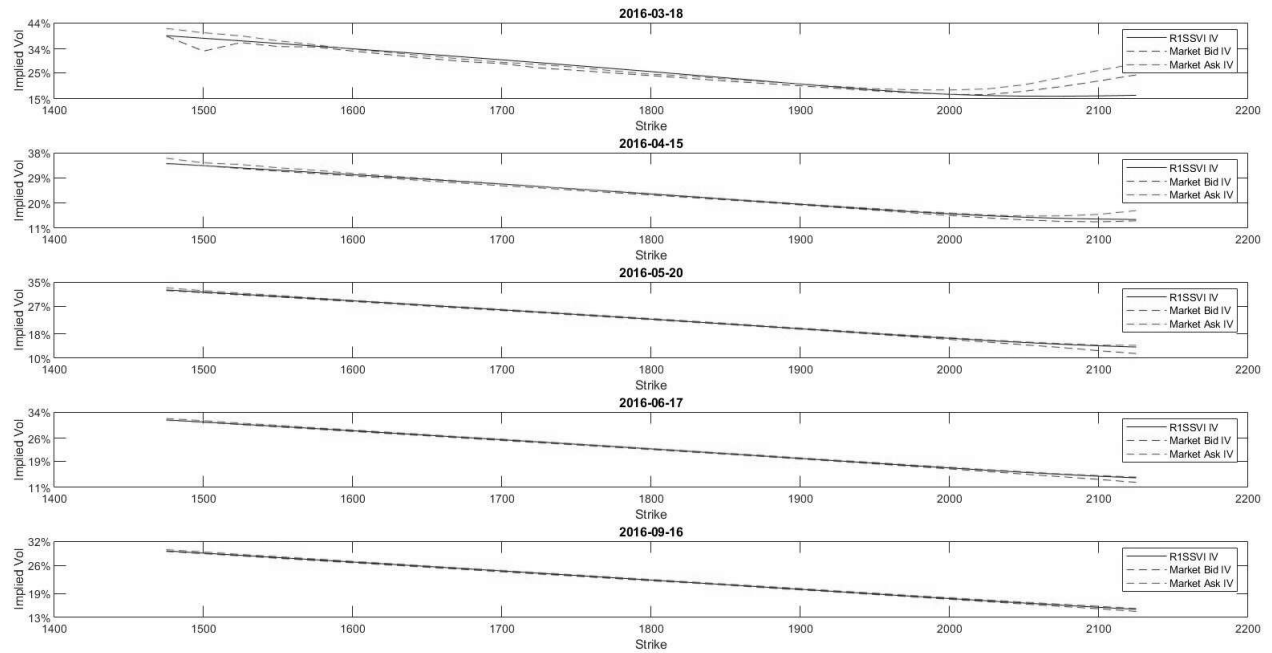


Figure 20: February 22nd, 2016 R1SSVI Implied Vol Fit Set 1

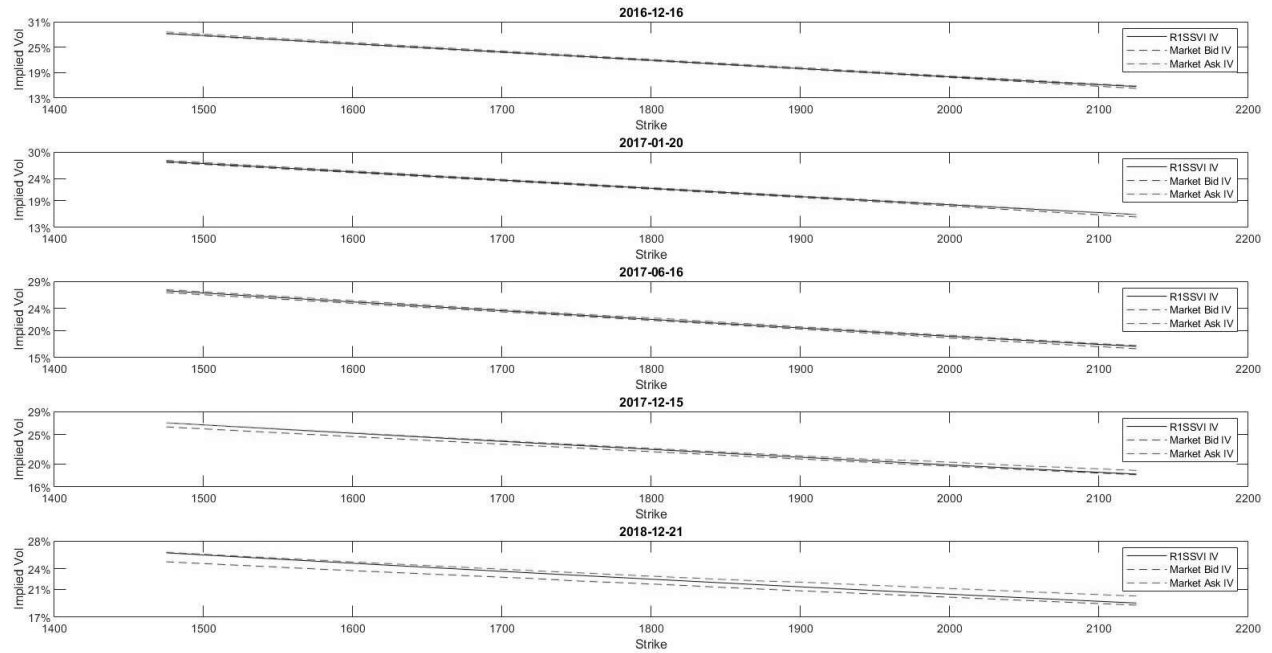


Figure 21: February 22nd, 2016 R1SSVI Implied Vol Fit Set 2

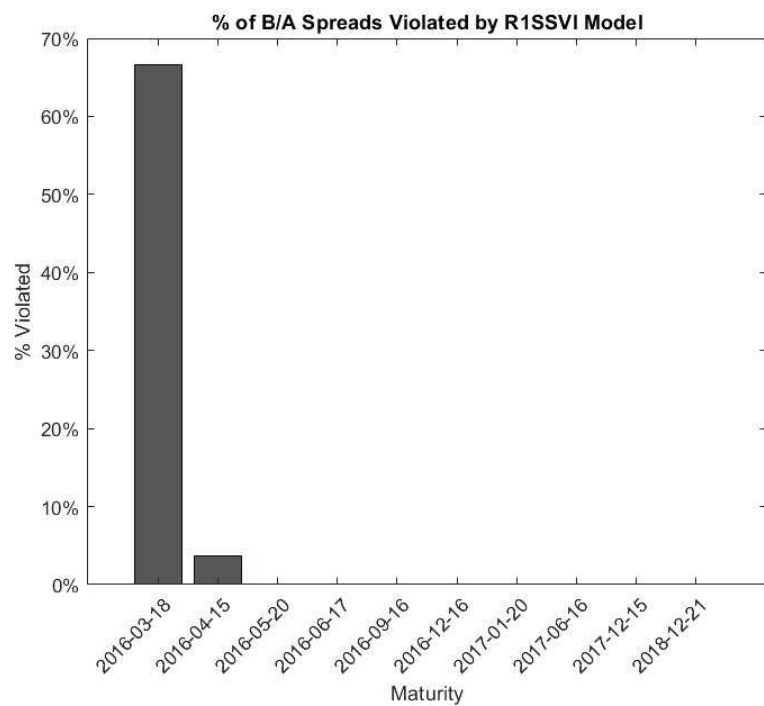


Figure 22: February 22nd, 2016 R1SSVI Implied Vol Fit Bid/Ask Spread Violations

### 5.4.2 R2 Model

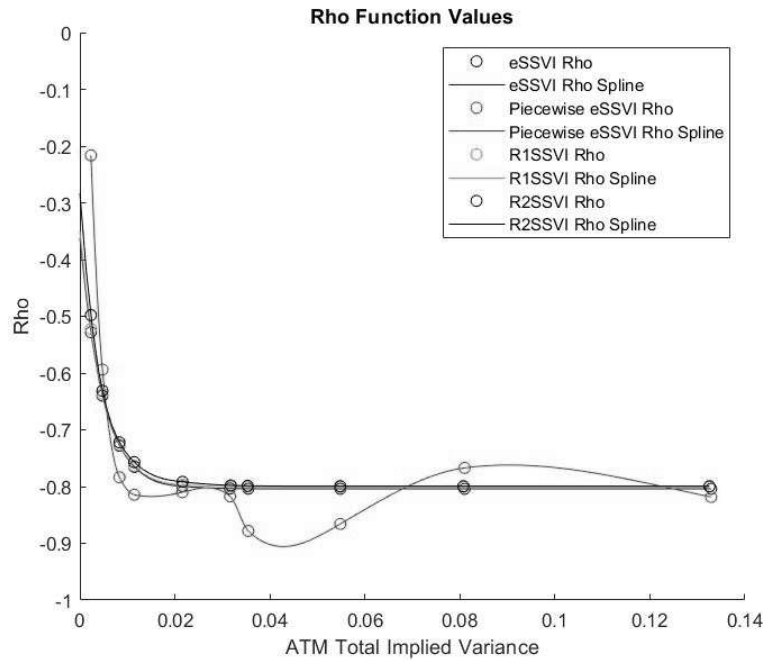


Figure 23: Rho Function Comparisons

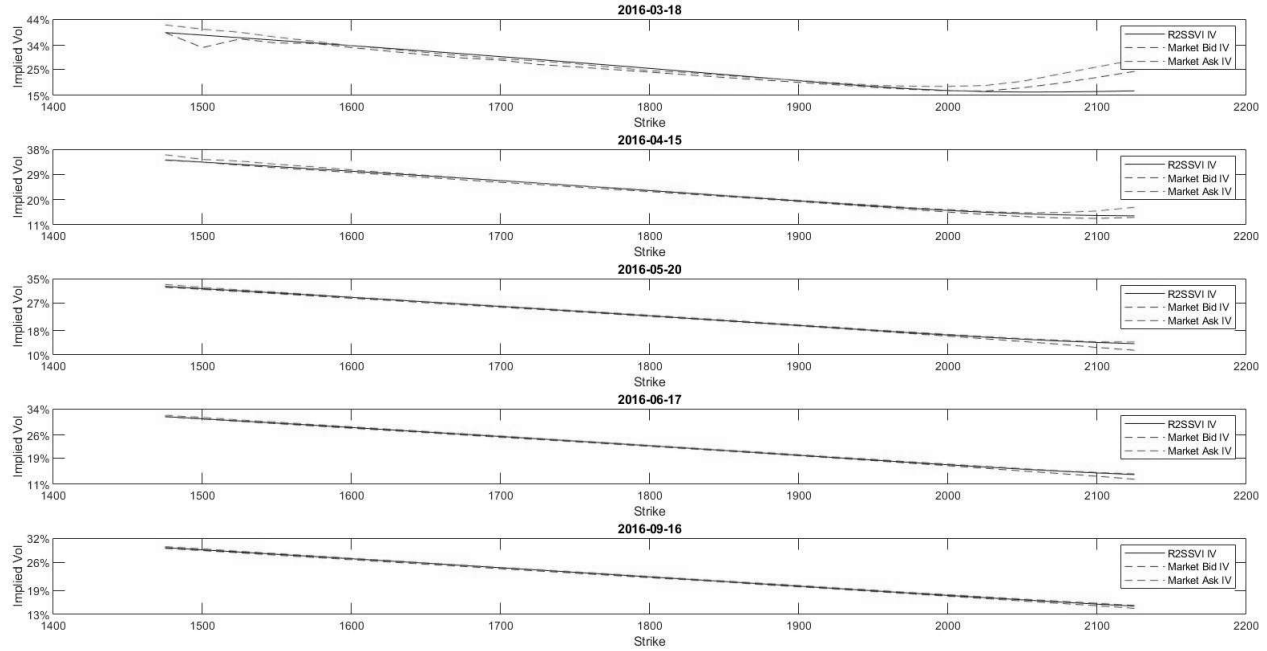


Figure 24: February 22nd, 2016 R2SSVI Implied Vol Fit Set 1

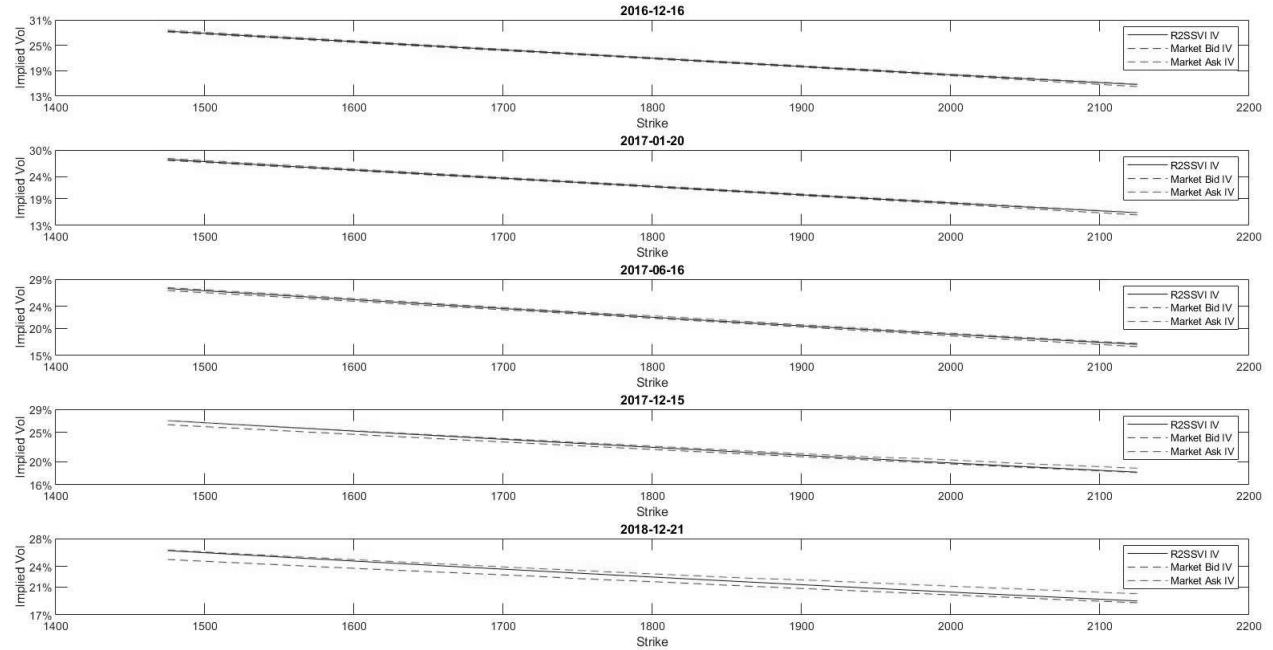


Figure 25: February 22nd, 2016 R2SSVI Implied Vol Fit Set 2

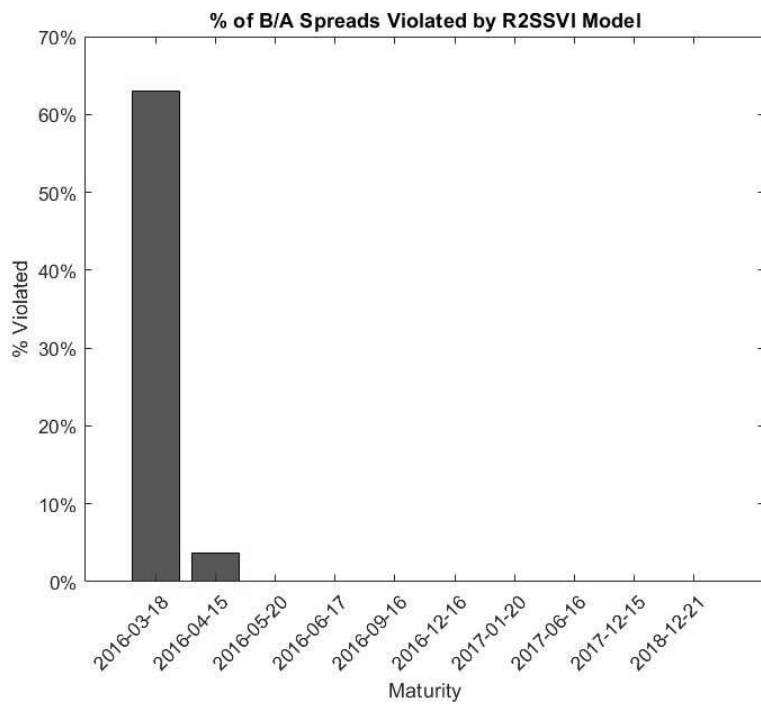


Figure 26: February 22nd, 2016 R2SSVI Implied Vol Fit Bid/Ask Spread Violations

### 5.4.3 R3 Model

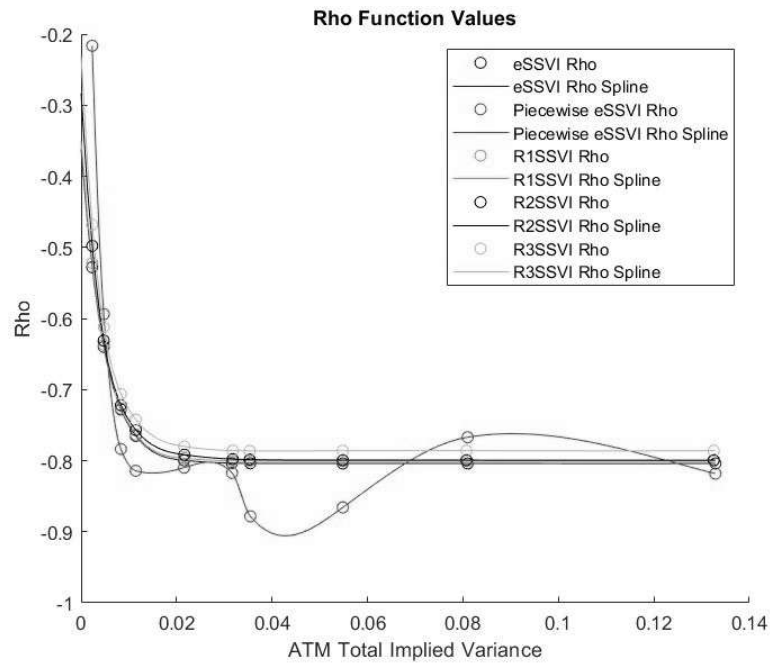


Figure 27: Rho Function Comparisons

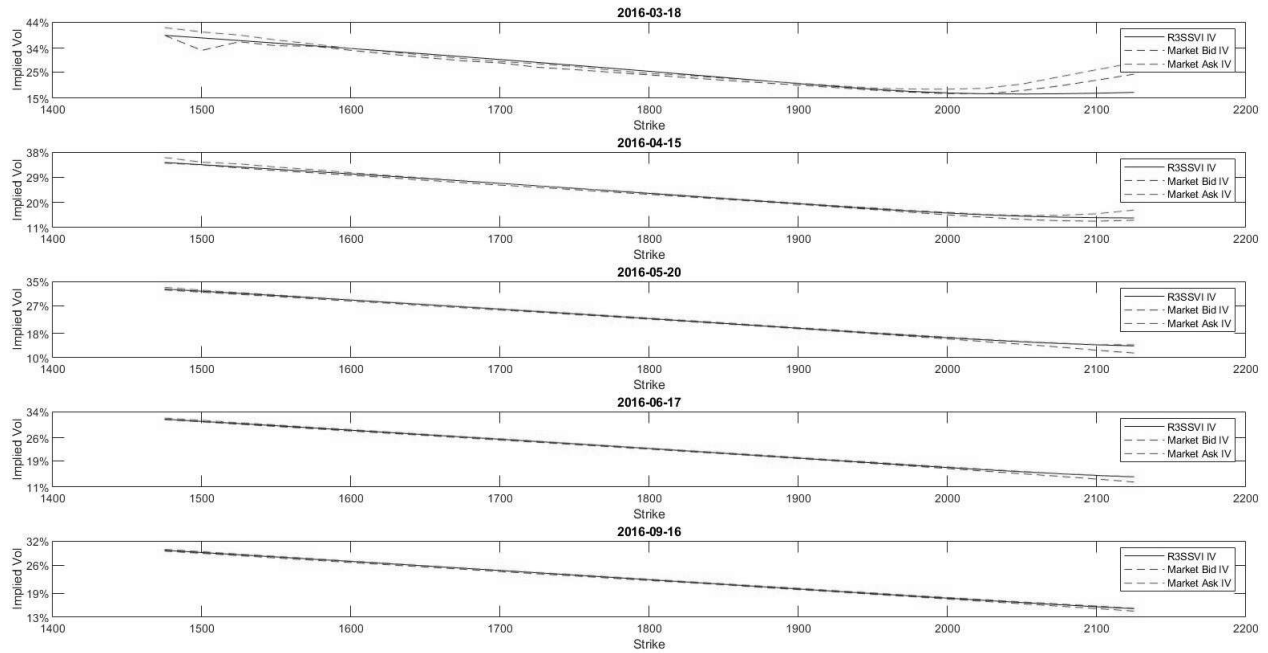


Figure 28: February 22nd, 2016 R3SSVI Implied Vol Fit Set 1

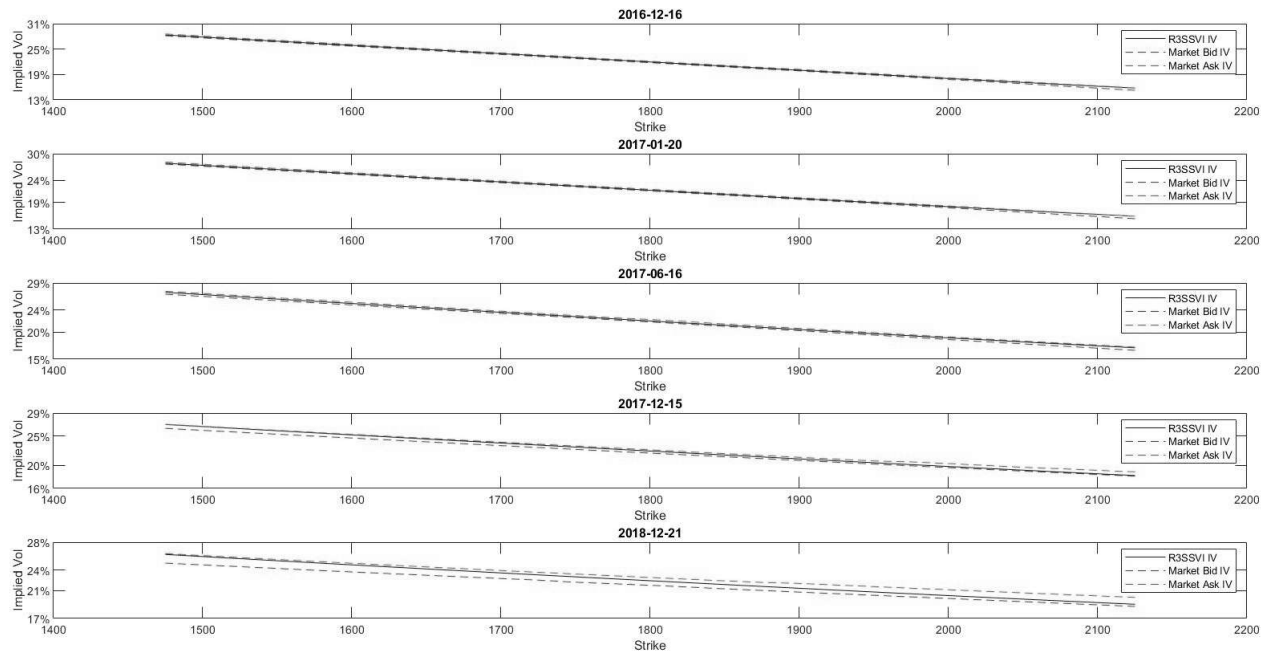


Figure 29: February 22nd, 2016 R3SSVI Implied Vol Fit Set 2

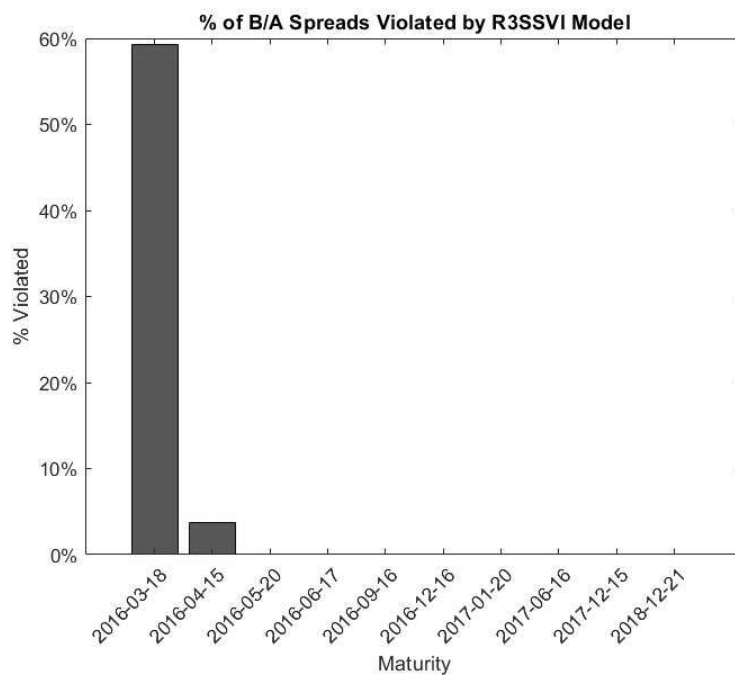


Figure 30: February 22nd, 2016 R3SSVI Implied Vol Fit Bid/Ask Spread Violations

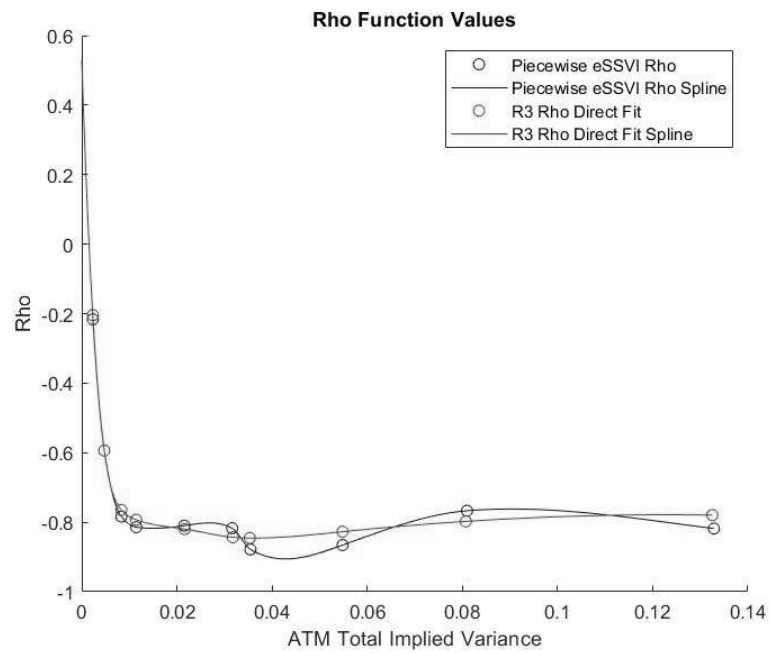


Figure 31: Direct Fit of R3 Rho Functional Form to Piecewise eSSVI Rho

## 6 Conclusion

This paper examined an extension to the (e)SSVI model of the implied volatility surface that attempted to capture the behavior inferred from maturity-specific or piecewise calibrations of existing parameterizations. It was found that although a functional form for the correlation between the underlying asset and its instantaneous volatility that more suitably reflects the oscillatory behavior implied by the maturity-wise calibrations can be found by a generalization of the eSSVI model (that is, we derived a form for  $\rho$  in which the eSSVI is a special case), the no-arbitrage constraints prove too restrictive to allow admissible parameterizations that take advantage of the offered flexibility. In the end, the higher order forms for  $\rho$  tend to collapse parametrically in such a way that their behavior across implied ATM total variance,  $\theta$ , matches closely that found for the eSSVI model. Still, there may be some hope for future research to find admissible models which incorporate the extensions developed herein. Consider that throughout we used the simple basic power law form for  $\varphi$ , or  $\varphi = \eta\theta_t^{-\lambda}$ . Alternative forms for this input that are consistent with the oscillatory behavior of the higher order Rx models, in the sense that they admit models with similar behavior as the piecewise models studied, could be discovered. Also, alternative approaches to the calibration methodology could allow us to better find admissible models. For example, it could be interesting to explore a sequential calibration which first fits a higher order Rx model directly to the piecewise derived behavior of  $\rho$ , similar to what was done in Section 5.4.3, then locks these parameters for a second calibration which attempts to find only values of  $\eta$  and  $\lambda$  which satisfy the no-arbitrage constraints.

## References

- [1] Bachelier, L., 1900. Théorie de la Spéculation. *Annales Scientifiques de l'École Normale Supérieure*. 3 (17):21-86.
- [2] Bakshi, G., Cao, C., Chen, Z., 1997. Empirical Performance of Alternative Option Pricing Models. *Journal of Finance*. 52:2003-2049.
- [3] Barndorff-Nielsen, O. E., 1995. Normal Inverse Gaussian Distributions and the Modeling of Stock Returns. Research Report no. 300, Department of Theoretical Statistics, Aarhus University.
- [4] Björk, T., 2009. Arbitrage Theory in Continuous Time, Third Edition. *Oxford University Press*.
- [5] Black, F., Scholes, M., 1973. The Pricing of Options and Corporate Liabilities. *The Journal of Political Economy*. 81:637-654.
- [6] Bookstaber, R., McDonald, J., 1987. A General Distribution for Describing Security Price Returns. *The Journal of Business*. 60:401-424.
- [7] Breeden, D. T., Litzenberger, R. H., 1978. Prices of State-Contingent Claims Implicit in Option Prices. *Journal of Business*. 51 (4):621-651.
- [8] Carr, P., Geman, H., Madan, D., Yor, M., 2002. The Fine Structure of Asset Returns: An Empirical Investigation. *Journal of Business* 75:305-332.
- [9] Carr, P., Madan, D., 2005. A Note on Sufficient Conditions for No Arbitrage. *Finance Research Letters* 2:125-130.
- [10] Cox, J., 1975. Notes on Option Pricing I: Constant Elasticity of Diffusions. Unpublished Draft, Stanford University, 1975.
- [11] Eberlein, E., Keller, U., 1995. Hyperbolic Distributions in Finance. *Bernoulli*. 1:281-299.
- [12] Gatheral, J., 2004. A Parsimonious Arbitrage-Free Implied Volatility Parameterization with Application to the Valuation of Volatility Derivatives. Presentation at Global Derivatives 2004.
- [13] Gatheral, J., 2006. The Volatility Surface, A Practitioner's Guide. Wiley Finance.
- [14] Gatheral, J., Jacquier, A., 2013. Arbitrage Free SVI Volatility Surfaces. *Quantitative Finance*. 14 (1):59-71.

- [15] Hagan, S., Kumar, D., Lesniewski, A., Woodward, D., 2002. Managing Smile Risk. *Wilmott*. 1:84-108.
- [16] Harrison, J. M., Pliska, S. R., 1981. Martingales and Stochastic Integrals in the Theory of Continuous Trading. *Stochastic Processes and Their Application*. 11:215-260.
- [17] Hendricks, S., 2016. Extending the SSVI Model with Arbitrage-Free Conditions. Masters Thesis, Delft University, 2016.
- [18] Hendricks, S., Martini, C., 2019. The Extended SSVI Volatility Surface. *Journal of Computational Finance*. 22:25-39.
- [19] Heston, S. L., 1993. A Closed-Form Solution for Options with Stochastic Volatility and Applications to Bond and Currency Options. *The Review of Financial Studies*. 6 (2):327-343.
- [20] Higgins, L., 1906. The Put-And-Call. The Aberdeen University Press Limited.
- [21] Hurn, A., Lindsay, K., Pavlov, V., 2005. Smooth Estimation of Yield Curves by Laguerre Functions. *MODSIM 05 - International Congress On Modelling And Simulation Advances And Applications For Management And Decision Making*. The Modelling and Simulation Society of Australia and New Zealand, Australia, pp. 1042-1048.
- [22] Kou, S. G., 2002. A Jump-Diffusion Model for Option Pricing. *Management Science*. 48 (8): 1086-1101.
- [23] Lee, R., 2004. The Moment Formula for Implied Volatility at Extreme Strikes. *Mathematical Finance*. 14 (3):469-480.
- [24] Madan, D., Seneta, E., 1990. The Variance Gamma (V.G.) Model for Share Market Returns. *The Journal of Business*. 63 (4):511-524.
- [25] Mandelbrot, B., 1963. New Methods in Statistical Economics. *The Journal of Political Economy*. 71 (5):421-440.
- [26] Merton, R. C., 1976. Option Pricing When Underlying Stock Returns are Discontinuous. *Journal of Financial Economics*. 3 (1-2):125-144.
- [27] Nelson, S. A., 1904. The ABC of Options and Arbitrage. Andesite Press.
- [28] Nelson, C., Siegel, A., 1987. Parsimonious Modeling of Yield Curves. *The Journal of Business*. 60 (4):473-489.
- [29] Praetz, P., 1972. The Distribution of Share Price Changes. *The Journal of Business*. 45:49-55.

- [30] Press, S., 1967. A Compound Event Model for Security Prices. *The Journal of Business*. 40:317-335.
- [31] Rogers, L., Tehranchi, M., 2010. Can the Implied Volatility Surface Move by Parallel Shifts? *Finance and Stochastics*. 14:235-248.
- [32] Rosenberg, J., Engle, R., 2002. Empirical Pricing Kernels. *Journal of Financial Economics*. 64:341-372.
- [33] Schoutens, W., 2001. The Meixner Process in Finance. EURANDOM Report 2001-002. EURANDOM, Eindhoven.
- [34] de Sousa, W., Matt, C., 2018. An Unconditionally Stable Laguerre Based Finite Difference Method for Transient Diffusion and Convection-Diffusion Problems. *Numerical Mathematics Theory Methods and Applications*. 12 (3).
- [35] Svensson, L. E., 1994. Estimating and Interpreting Forward Interest Rates: Sweden 1992-1994. Discussion Paper 1051, Centre for Economic Policy Research.

# Appendices

## A The Black-Scholes Model

Any implied volatility model is inextricably linked to the Black-Scholes framework. After all, implied volatility is just the inversion of the Black-Scholes solution in  $\sigma$ , the volatility parameter. Understanding the underlying pricing model is therefore exceedingly beneficial in parsing the efforts being made to model this single yet highly consequential number. Due mainly to a long-standing desire to formalize my own notes on the Black-Scholes model, this appendix derives and solves in great detail the classical problem of pricing simple European options using the model. All that follows assumes the underlying asset does not pay a dividend, although including proportional dividends is relatively straightforward.

### A.1 Derivation of the PDE for a Non-Dividend Paying Asset

Consider a contingent claim denoted  $\Phi(S_T)$  (i.e. the payoff function) with pricing function  $F(t, S_t) = \pi_t$ . Let the stock price and bank account dynamics be given by a geometric Brownian motion and completely deterministic function, respectively, as

$$dS_t = \alpha S_t dt + \sigma S_t dW_t, \quad (\text{A.1})$$

$$dB_t = r B_t dt. \quad (\text{A.2})$$

The value process (of a portfolio of the underlying stock and the option written on the underlying) is given by

$$V_t = h_t^s S_t + h_t^\pi \pi$$

$$\implies dV_t = h_t^s dS_t + h_t^\pi d\pi, \quad (\text{A.3})$$

where  $h_t^s$  and  $h_t^\pi$  denote the number of shares of stock at time  $t$  and the number of options at time  $t$ , respectively. Since these are equal to  $\frac{w_t^s V}{S_t}$  and  $\frac{V w_t^\pi}{\pi}$ , where  $w_t^s$  and  $w_t^\pi$  represent the weight of the portfolio allocated to the underlying asset and the option, respectively, we thus have

$$dV_t = V \left( w_t^s \frac{dS_t}{S_t} + w_t^\pi \frac{d\pi}{\pi} \right). \quad (\text{A.4})$$

Applying Ito's formula to  $F(t, S_t)$ , we have

$$dF = \frac{\partial F}{\partial t} dt + \frac{\partial F}{\partial S} dS_t + \frac{1}{2} \frac{\partial^2 F}{\partial S^2} (dS_t)^2. \quad (\text{A.5})$$

Plugging in the dynamics for  $S_t$  from Equation (A.1) yields

$$dF = \frac{\partial F}{\partial t} dt + \frac{\partial F}{\partial S} (\alpha S_t dt + \sigma S_t dW_t) + \frac{1}{2} \frac{\partial^2 F}{\partial S^2} \sigma^2 S_t^2 dt. \quad (\text{A.6})$$

Multiply and divide everything by  $F$  and simplify notation as

$$\begin{aligned} dF &= F \underbrace{\left( \frac{\partial F}{\partial t} + \frac{\partial F}{\partial S} \alpha S_t + \frac{1}{2} \frac{\partial^2 F}{\partial S^2} \sigma^2 S_t^2 \right)}_{\alpha_F} dt + F \underbrace{\frac{\partial F}{\partial S} S_t \sigma}_{\sigma_F} dW_t \\ &\Leftrightarrow dF = \alpha_F F dt + \sigma_F F dW_t. \end{aligned} \quad (\text{A.7})$$

Since  $F$  is the pricing function, we take  $F = \pi$ , and thus

$$\frac{d\pi}{\pi} = \alpha_F dt + \sigma_F dW_t. \quad (\text{A.8})$$

Using this along with the assumed stock dynamics of Equation (A.1), we can now go back to the value dynamics of Equation (A.4) and plug in the results for  $dS_t$  and  $\frac{d\pi}{\pi}$ , giving

$$dV_t = V \left( w^s \frac{\alpha S_t dt + \sigma S_t dW_t}{S_t} + w^\pi (\alpha_F dt + \sigma_F dW_t) \right) \quad (\text{A.9})$$

$$\Leftrightarrow dV_t = V \cdot \underbrace{(w^s \alpha + w^\pi \alpha_F)}_{=r \text{ to avoid arbitrage}} dt + V \cdot \underbrace{(w^s \sigma + w^\pi \sigma_F)}_{=0 \text{ for no risk}} dW_t. \quad (\text{A.10})$$

The conditions in underbraces, along with the condition that portfolio weights must sum to 1 thus leads to the following system of equations:

$$\begin{cases} w^s\alpha + w^\pi\alpha_F = r \\ w^s\sigma + w^\pi\sigma_F = 0 \\ w^s + w^\pi = 1 \end{cases} \quad (\text{A.11})$$

The first equation will lead to the PDE, so begin working through the first two:

$$\begin{aligned} w^s = 1 - w^\pi &\implies (1 - w^\pi)\sigma + w^\pi\sigma_F = 0 \Leftrightarrow \sigma - w^\pi\sigma + w^\pi\sigma_F = 0 \\ &\Leftrightarrow w^\pi(\sigma_F - \sigma) = -\sigma \Leftrightarrow w^\pi = \frac{-\sigma}{\sigma_F - \sigma} \Leftrightarrow \\ &w^\pi = \frac{\sigma}{\sigma - \sigma_F}. \end{aligned} \quad (\text{A.12})$$

$$\begin{aligned} w^s + \frac{\sigma}{\sigma - \sigma_F} = 1 &\Leftrightarrow w^s = 1 - \frac{\sigma}{\sigma - \sigma_F} = \frac{\sigma - \sigma_F}{\sigma - \sigma_F} - \frac{\sigma}{\sigma - \sigma_F} = \frac{-\sigma_F}{\sigma - \sigma_F} \Leftrightarrow \\ &w^s = \frac{\sigma_F}{\sigma_F - \sigma}. \end{aligned} \quad (\text{A.13})$$

Now, plugging equations (A.12) and (A.13) into the first equation of the system of equation (A.13) yields

$$\begin{aligned} \frac{\sigma_F\alpha}{\sigma_F - \sigma} + \frac{\sigma\alpha_F}{\sigma - \sigma_F} = r &\Leftrightarrow \frac{\sigma_F\alpha}{\sigma_F - \sigma} - \frac{\sigma\alpha_F}{\sigma_F - \sigma} = r \Leftrightarrow \sigma_F\alpha - \sigma\alpha_F = r(\sigma_F - \sigma) \Leftrightarrow \\ \sigma_F\alpha - \sigma\alpha_F = r\sigma_F - r\sigma &\Leftrightarrow \sigma_F\alpha - \sigma_Fr = \sigma\alpha_F - \sigma r \Leftrightarrow \sigma_F(\alpha - r) = \sigma(\alpha_F - r) \Leftrightarrow \\ \frac{\alpha - r}{\sigma} &= \frac{\alpha_F - r}{\sigma_F}. \end{aligned} \quad (\text{A.14})$$

The interpretation of this result is that the market price of risk (MPR) for each asset (underlying and option) is equivalent! Allow the MPR for the underlying to equal  $\lambda$ , that is,

$$\lambda = \frac{\alpha - r}{\sigma} = \frac{\alpha_F - r}{\sigma_F} \Leftrightarrow \lambda\sigma_F = \alpha_F - r. \quad (\text{A.15})$$

Plug in the original expressions for  $\alpha_F$  and  $\sigma_F$  from equation (A.7) into this equation to get

$$\begin{aligned} \lambda \frac{\frac{\partial F}{\partial S} S_t \sigma}{F} &= \frac{\frac{\partial F}{\partial t} + \frac{\partial F}{\partial S} \alpha S_t + \frac{1}{2} \sigma^2 S_t^2 \frac{\partial^2 F}{\partial S^2}}{F} - r \Leftrightarrow \\ \lambda \frac{\partial F}{\partial S} S_t \sigma &= \frac{\partial F}{\partial t} + \frac{\partial F}{\partial S} \alpha S_t + \frac{1}{2} \sigma^2 S_t^2 \frac{\partial^2 F}{\partial S^2} - rF \Leftrightarrow \\ \frac{\partial F}{\partial t} + \frac{\partial F}{\partial S} \alpha S_t - \lambda \frac{\partial F}{\partial S} S_t \sigma + \frac{1}{2} \sigma^2 S_t^2 \frac{\partial^2 F}{\partial S^2} - rF &= 0 \Leftrightarrow \\ \frac{\partial F}{\partial t} + \frac{\partial F}{\partial S} (\alpha - \lambda\sigma) S_t + \frac{1}{2} \sigma^2 S_t^2 \frac{\partial^2 F}{\partial S^2} - rF &= 0. \end{aligned} \quad (\text{A.16})$$

Finally, recall from Equation (A.15) that  $\lambda = \frac{\alpha-r}{\sigma}$  and plug this in, yielding

$$\begin{aligned} \frac{\partial F}{\partial t} + \frac{\partial F}{\partial S} \left( \alpha - \left( \frac{\alpha-r}{\sigma} \right) \sigma \right) S_t + \frac{1}{2} \sigma^2 S_t^2 \frac{\partial^2 F}{\partial S^2} - rF &= 0 \Leftrightarrow \\ \frac{\partial F}{\partial t} + r \frac{\partial F}{\partial S} S_t + \frac{1}{2} \sigma^2 S_t^2 \frac{\partial^2 F}{\partial S^2} - rF &= 0, \end{aligned} \quad (\text{A.17})$$

which is the Black-Scholes PDE for a non-dividend paying asset.

## A.2 Change of Measure for a Non-Dividend Paying Asset

Using the Girsanov theorem, we will now derive the  $\mathbb{Q}$ -dynamics of non-dividend paying asset  $S$  by changing measure from  $\mathbb{P}$  to  $\mathbb{Q}$  and also derive the  $\mathbb{Q}_S$ -dynamics of  $S$  by changing measure from  $\mathbb{Q}$  to  $\mathbb{Q}_S$ . These become important for when we later solve the PDE derived above. As before, consider the price dynamics for the underlying under the real world probability measure  $\mathbb{P}$  along with the bank account dynamics as a geometric Brownian motion and completely

deterministic function, respectively:

$$dS_t = \alpha S_t dt + \sigma S_t dW_t, \quad (\text{A.18})$$

$$dB_t = r B_t dt. \quad (\text{A.19})$$

Consider another process for the stock price dynamics with the bank account as the numeraire or denominator, otherwise known as the discounted price process  $\frac{S_t}{B_t}$  since the solution of Equation (A.19) would yield  $B_t = e^{rt}$ . Now, it is important to remember the full Ito quotient rule,

$$d\left(\frac{x}{y}\right) = \frac{x}{y}\left(\frac{dx}{x} - \frac{dy}{y}\right) - \frac{dx \cdot dy}{xy} + \left(\frac{dy}{y}\right)^2. \quad (\text{A.20})$$

Thus, we have

$$d\left(\frac{S_t}{B_t}\right) = \frac{S_t}{B_t}\left(\frac{dS_t}{S_t} - \frac{dB_t}{B_t}\right) - \frac{dS_t dB_t}{S_t B_t} + \left(\frac{dB_t}{B_t}\right)^2. \quad (\text{A.21})$$

Utilizing the dynamics from Equations (A.18) and (A.19), we have

$$d\left(\frac{S_t}{B_t}\right) = \frac{S_t}{B_t}\left(\frac{\alpha S_t dt + \sigma S_t dW_t}{S_t} - \frac{r B_t dt}{B_t}\right) - \frac{(\alpha S_t dt + \sigma S_t dW_t)r B_t dt}{S_t B_t} + \left(\frac{r B_t dt}{B_t}\right)^2, \quad (\text{A.22})$$

where, note that the last two terms equal zero due to the Ito multiplication rules, which tell us that any  $dt^2$  and  $dt dW_t$  (equivalently  $dW_t dt$ ) terms cancel, and only  $dW_t^2 \approx dt$ . Thus, we have

$$\begin{aligned} d\left(\frac{S_t}{B_t}\right) &= \frac{S_t}{B_t}(\alpha dt + \sigma dW_t - r dt) \\ \Leftrightarrow d\left(\frac{S_t}{B_t}\right) &= \frac{\alpha S_t dt + \sigma S_t dW_t}{B_t} - \frac{r S_t dt}{B_t}, \end{aligned}$$

which we can write as

$$d\left(\frac{S_t}{B_t}\right) = \frac{\alpha S_t dt + \sigma S_t dW_t}{B_t} - \frac{S_t}{(B_t)^2} r B_t dB_t. \quad (\text{A.23})$$

Continuing on,

$$\begin{aligned} d\left(\frac{S_t}{B_t}\right) &= \frac{\alpha S_t dt + \sigma S_t dW_t}{B_t} - \frac{S_t}{(B_t)^2}(r B_t dt) = \frac{1}{B_t} \alpha S_t dt + \frac{1}{B_t} \sigma S_t dW_t - \frac{1}{B_t} r S_t dt \\ &= \frac{1}{B_t} (\alpha - r) S_t dt + \frac{1}{B_t} \sigma S_t dW_t. \end{aligned} \quad (\text{A.24})$$

Now, all importantly, by Girsanov's theorem, we have that

$$dW_t = \varphi dt + dW_t^{\mathbb{Q}}. \quad (\text{A.25})$$

Plugging this result into Equation (A.24) yields

$$\begin{aligned} d\left(\frac{S_t}{B_t}\right) &= \frac{1}{B_t} (\alpha - r) S_t dt + \frac{1}{B_t} \sigma S_t (\varphi dt + dW_t^{\mathbb{Q}}) \\ &= \frac{1}{B_t} (\alpha - r + \sigma \varphi) S_t dt + \frac{1}{B_t} \sigma S_t dW_t^{\mathbb{Q}}. \end{aligned} \quad (\text{A.26})$$

Now, to make this last process a  $\mathbb{Q}$ -martingale, we need the  $dt$  term (drift) to disappear. We can do this by setting the coefficient to zero,

$$\alpha - r + \sigma \varphi = 0 \Leftrightarrow \varphi = \frac{r - \alpha}{\sigma}. \quad (\text{A.27})$$

This is thus the Girsanov kernel. Now we revisit the original price dynamics for the stock, and invoke Girsanov's theorem as noted before in Equation (A.25) but now with this derived kernel rather than the abstract kernel  $\varphi$  to yield

$$\begin{aligned} dS_t &= \alpha S_t dt + \sigma S_t \left( \frac{r - \alpha}{\sigma} dt + dW_t^{\mathbb{Q}} \right) \Leftrightarrow \\ dS_t &= (\alpha + r - \alpha) S_t dt + \sigma S_t dW_t^{\mathbb{Q}} \Leftrightarrow \\ dS_t &= r S_t dt + \sigma S_t dW_t^{\mathbb{Q}}. \end{aligned} \quad (\text{A.28})$$

These are thus the  $\mathbb{Q}$ -dynamics of  $S$ .

Now, moving on to the  $\mathbb{Q}_{\mathbb{S}}$ -dynamics of  $S$ . In this case, we will consider instead the stock as the numeraire of the bond process, or  $\frac{B_t}{S_t}$ . For ease of reading, we reproduce the Ito quotient rule,

$$d\left(\frac{x}{y}\right) = \frac{x}{y}\left(\frac{dx}{x} - \frac{dy}{y}\right) - \frac{dx \cdot dy}{xy} + \left(\frac{dy}{y}\right)^2, \quad (\text{A.29})$$

and, importantly, we are starting from the  $\mathbb{Q}$ -dynamics of  $S$  as found above. Thus, we have

$$d\left(\frac{B_t}{S_t}\right) = \frac{B_t}{S_t}\left(\frac{dB_t}{B_t} - \frac{dS_t}{S_t} - \frac{dS_t dB_t}{S_t B_t} + \left(\frac{dS_t}{S_t}\right)^2\right). \quad (\text{A.30})$$

Utilizing the  $\mathbb{Q}$ -dynamics of  $S$  and the dynamics of  $B$  (and knowing that the cross-term must cancel again), we have

$$\begin{aligned} d\left(\frac{B_t}{S_t}\right) &= \frac{B_t}{S_t}\left(\frac{r\cancel{B}_t dt}{\cancel{B}_t} - \frac{r\cancel{S}_t dt + \sigma\cancel{S}_t dW_t^{\mathbb{Q}}}{\cancel{S}_t} + \left(\frac{r\cancel{S}_t dt + \sigma\cancel{S}_t dW_t^{\mathbb{Q}}}{\cancel{S}_t}\right)^2\right) \\ &\Leftrightarrow d\left(\frac{B_t}{S_t}\right) = \frac{B_t}{S_t}(rdt - rdt - \sigma dW_t^{\mathbb{Q}} + \sigma^2 dt) \\ &\Leftrightarrow d\left(\frac{B_t}{S_t}\right) = \frac{B_t}{S_t}\sigma^2 dt - \frac{B_t}{S_t}\sigma dW_t^{\mathbb{Q}}. \end{aligned} \quad (\text{A.31})$$

By Girsanov's theorem, we have that  $dW_t^{\mathbb{Q}} = \varphi^S dt + dW_t^{\mathbb{Q}_{\mathbb{S}}}$ . Plugging this result in yields

$$\begin{aligned} &\Leftrightarrow d\left(\frac{B_t}{S_t}\right) = \frac{B_t}{S_t}\sigma^2 dt - \frac{B_t}{S_t}\sigma[\varphi^S dt + dW_t^{\mathbb{Q}_{\mathbb{S}}}] \\ &\Leftrightarrow d\left(\frac{B_t}{S_t}\right) = \frac{B_t}{S_t}(\sigma^2 dt - \sigma\varphi^S) - \frac{B_t}{S_t}\sigma dW_t^{\mathbb{Q}_{\mathbb{S}}}. \end{aligned} \quad (\text{A.32})$$

Now, to make this last process a  $\mathbb{Q}_{\mathbb{S}}$ -martingale, we need the  $dt$  term (drift) to disappear as before, that is

$$\sigma^2 - \sigma\varphi^S = 0 \Leftrightarrow \varphi^S = \sigma. \quad (\text{A.33})$$

This is thus the Girsanov kernel. Going back to the  $\mathbb{Q}$ -dynamics of  $S$  and plugging this result in yields

$$\begin{aligned} dS_t &= rS_t dt + \sigma S_t [\sigma dt + dW_t^{\mathbb{Q}_S}] \\ \Leftrightarrow dS_t &= (r + \sigma^2)S_t dt + \sigma S_t dW_t^{\mathbb{Q}_S}. \end{aligned} \quad (\text{A.34})$$

These are thus the  $\mathbb{Q}_S$ -dynamics of  $S$ .

### A.3 Solution to the Stochastic Dynamics of a Non-Dividend Paying Asset

This section solves the stochastic differential equations (SDEs) for the  $\mathbb{Q}$ -dynamics and the  $\mathbb{Q}_S$ -dynamics of non-dividend paying asset  $S$  as found above. These solutions become important for when we later solve the PDE derived above. Recall that under the measure  $\mathbb{Q}$ , we found

$$dS_t = rS_t dt + \sigma dW_t^{\mathbb{Q}}. \quad (\text{A.35})$$

Apply Ito's formula to the function  $f = \ln(x)$ . This yields (note there is no time dimension)

$$df = \frac{1}{x}dx - \frac{1}{2}\frac{1}{x^2}(dx)^2, \quad (\text{A.36})$$

which implies that

$$d\ln(S_t) = \frac{1}{S_t}dS_t - \frac{1}{2}\frac{1}{S_t^2}(dS_t)^2. \quad (\text{A.37})$$

Plugging in the  $\mathbb{Q}$ -dynamics of  $S$  (Equation (A.28)) yields (note the Ito product rule was used to quickly get to the last term)

$$d\ln(S_t) = \frac{1}{S_t}(rS_t dt + \sigma S_t dW_t^{\mathbb{Q}}) - \frac{1}{2}\frac{1}{S_t^2}\sigma^2 S_t^2 dt \quad (\text{A.38})$$

$$\Leftrightarrow d\ln(S_t) = (r - \frac{1}{2}\sigma^2)dt + \sigma dW_t^{\mathbb{Q}}. \quad (\text{A.39})$$

Integrating,

$$\ln(S_T) - \ln(S_t) = \int_t^T (r - \frac{1}{2}\sigma^2)dt + \int_t^T \sigma dW_t^{\mathbb{Q}}$$

$$\Leftrightarrow \ln(S_T) = \ln(S_t) + (r - \frac{1}{2}\sigma^2)(T - t) + \sigma W_{T-t}^{\mathbb{Q}}. \quad (\text{A.40})$$

Finally, exponentiating both sides gives

$$S_T = e^{\ln(S_t) + (r - \frac{1}{2}\sigma^2)(T - t) + \sigma W_{T-t}^{\mathbb{Q}}}, \quad (\text{A.41})$$

which we can write as

$$S_T = S_t e^{(r - \frac{1}{2}\sigma^2)(T - t) + \sigma W_{T-t}^{\mathbb{Q}}}. \quad (\text{A.42})$$

This is thus the solution to the geometric Brownian motion SDE under the  $\mathbb{Q}$ -dynamics. Without going through all the same math, we can thus infer that the solution to the SDE under the  $\mathbb{Q}_S$ -dynamics is

$$S_T = S_t e^{(r - \frac{1}{2}\sigma^2 + \sigma^2)(T - t) + \sigma W_{T-t}^{\mathbb{Q}}} \quad (\text{A.43})$$

$$\Leftrightarrow S_T = S_t e^{(r + \frac{1}{2}\sigma^2)(T - t) + \sigma W_{T-t}^{\mathbb{Q}_S}}. \quad (\text{A.44})$$

## A.4 Solution to the PDE by the Feynman-Kac Formula

This section solves the Black Scholes PDE for a non-dividend paying asset as derived above using the Feynman-Kac formula. We will utilize the  $\mathbb{Q}$ -dynamics and the  $\mathbb{Q}_S$ -dynamics of a non-dividend paying asset  $S$  as found in Section A.2, along with the solution to these SDEs as found in the previous section. We will start with some detail of the Feynman-Kac formula. For this section, we will keep the same notation as can be found on for instance Wikipedia, and then draw the proper analogies and change notation as necessary for our problem. The Feynman-Kac formula says that the solution to a parabolic partial differential equation (PDE) of the form

$$\frac{\partial u}{\partial t}(x, t) + \mu(x, t) + \frac{1}{2}\sigma^2(x, t)\frac{\partial^2 u}{\partial x^2}(x, t) - V(x, t)u(x, t) + f(x, t) = 0, \quad (\text{A.45})$$

for all  $x \in \mathbb{R}$  and  $t \in [0, T]$  and subject to the terminal condition

$$u(x, T) = \psi(x), \quad (\text{A.46})$$

can be written as a conditional expectation

$$u(x, t) = \mathbb{E}^{\mathbb{Q}} \left[ \int_t^T e^{-\int_t^r V(X_{\tau}, \tau) d\tau} f(X_r, r) dr + e^{-\int_t^T V(X_{\tau}, \tau) d\tau} \psi(X_T) | X_t = x \right], \quad (\text{A.47})$$

under the appropriate probability measure  $\mathbb{Q}$  that gives  $X$  as an Ito process driven by the equation

$$dX = \mu(X, t) dt + \sigma(X, t) dW_t^{\mathbb{Q}}, \quad (\text{A.48})$$

with  $W_t^{\mathbb{Q}}$  a Weiner process under the measure  $Q$  and the initial condition  $X_t = x$ . Note that moving forward we will use the more succinct notation

$$\mathbb{E}_{t,x}^{\mathbb{Q}}[\cdot] = \mathbb{E}^{\mathbb{Q}}[\cdot | X_t = x]. \quad (\text{A.49})$$

Now let's map this notation to our problem for the Black-Scholes PDE for a non-dividend paying asset. First, we have

$$f(x, t) = 0. \quad (\text{A.50})$$

Also, for our purposes we have

$$u = F = \pi, \quad (\text{A.51})$$

$$V(x, t) = r, \quad (\text{A.52})$$

$$\psi(X_T) = \Phi(S_T) = \max(S_T - K, 0) = (S_T - K)^+, \quad (\text{A.53})$$

$$e^{-\int_t^T V(X_{\tau}, \tau) d\tau} = e^{-\int_t^T r d\tau} = e^{-r(T-t)}. \quad (\text{A.54})$$

So, pulling all of this together, we can say that the solution to the parabolic partial differential for a contingent claim on a non-dividend paying asset with terminal condition

$$\Phi(S_T) = (S_T - K)^+, \quad (\text{A.55})$$

is given by the conditional expectation

$$\pi(t, s) = \mathbb{E}_{t,s}^{\mathbb{Q}} \left[ e^{-r(T-t)} \Phi(S_T) \right], \quad (\text{A.56})$$

with dynamics for  $S$  given by the appropriate Ito process under  $Q$ , which we know from Equation (A.28) to be

$$dS_t = rS_t dt + \sigma S_t dW_t^{\mathbb{Q}}. \quad (\text{A.57})$$

First, we can rewrite the conditional expectation as

$$\begin{aligned} \pi(t, s) &= \mathbb{E}_{t,s}^{\mathbb{Q}} \left[ e^{-r(T-t)} (S_T - K)^+ \right] \\ \Leftrightarrow \pi(t, s) &= \mathbb{E}_{t,s}^{\mathbb{Q}} \left[ e^{-r(T-t)} S_T \chi_{\{S_T \geq K\}} \right] - \mathbb{E}_{t,s}^{\mathbb{Q}} \left[ e^{-r(T-t)} K \chi_{\{S_T \geq K\}} \right], \end{aligned} \quad (\text{A.58})$$

where  $\chi_z$  denotes the indicator function given condition  $z$ . Now, we will solve these separately, that is, consider the equations

$$\pi_{t,s}^1 = \mathbb{E}_{t,s}^{\mathbb{Q}} \left[ e^{-r(T-t)} S_T \chi_{\{S_T \geq K\}} \right], \quad (\text{A.59})$$

$$\pi_{t,s}^2 = -\mathbb{E}_{t,s}^{\mathbb{Q}} \left[ e^{-r(T-t)} K \chi_{\{S_T \geq K\}} \right], \quad (\text{A.60})$$

and in the end we can just recombine these as

$$\pi_{t,s} = \pi_{t,s}^1 + \pi_{t,s}^2. \quad (\text{A.61})$$

$\pi_{t,s}^2$  is a bit easier to solve than  $\pi_{t,s}^1$ , so we will start there. In fact, it might be good to take a moment to realize what we have by the decomposition above.  $\pi_{t,s}^1$  is really an asset-or-nothing binary option.  $\pi_{t,s}^2$  is really a cash-or-nothing binary option, as we can move  $K$  outside of the expectation and treat this like the cash payoff of the claim. That is, we can write

$$\pi_{t,s}^2 = -K e^{-r(T-t)} \mathbb{E}_{t,s}^{\mathbb{Q}} \left[ \chi_{\{S_T \geq K\}} \right]. \quad (\text{A.62})$$

The expectation of an indicator function is simply the probability of the even occurring, in this case  $S_T \geq K$ , and importantly under the  $\mathbb{Q}$ -probability. So, let's write this as

$$\pi_{t,s}^2 = -Ke^{-r(T-t)}\mathbb{Q}\left[S_T \geq K\right], \quad (\text{A.63})$$

where we're just using  $\mathbb{Q}[\cdot]$  to denote probability similar to the familiar  $\mathbb{P}[\cdot]$  but to emphasize the  $\mathbb{Q}$ -measure. Now, recall from the previous section what  $S_T$  is under  $\mathbb{Q}$ . For convenience, this is reproduced here from Equation (A.42),

$$S_T = S_t e^{(r-\frac{1}{2}\sigma^2)(T-t)+\sigma W_{T-t}^{\mathbb{Q}}}. \quad (\text{A.64})$$

Accordingly,

$$\pi_{t,s}^2 = -Ke^{-r(T-t)}\mathbb{Q}\left[S_t e^{(r-\frac{1}{2}\sigma^2)(T-t)+\sigma W_{T-t}^{\mathbb{Q}}} \geq K\right]. \quad (\text{A.65})$$

Now, focusing on the inequality term in brackets, if we first divide both sides by  $S_t$  (and obviously assuming  $S_t > 0$ ), then take logs of both sides and rearrange, we can write

$$\pi_{t,s}^2 = -Ke^{-r(T-t)}\mathbb{Q}\left[\sigma W_{T-t}^{\mathbb{Q}} \geq \ln(\frac{K}{S_t}) - (r - \frac{1}{2}\sigma^2)(T - t)\right]. \quad (\text{A.66})$$

Noting that  $\sigma W_{T-t}^{\mathbb{Q}} \sim N(0, \sigma^2(T-t))$ , standardizing the random variable as  $\gamma = (\sigma W_{T-t}^{\mathbb{Q}} - 0)/(\sigma\sqrt{T-t})$  and flipping the inequality results in

$$\begin{aligned} \pi_{t,s}^2 &= -Ke^{-r(T-t)}\mathbb{Q}\left[\gamma \leq \frac{\ln(\frac{S_t}{K}) + (r - \frac{1}{2}\sigma^2)(T - t)}{\sigma\sqrt{T-t}}\right] \Leftrightarrow \\ \pi_{t,s}^2 &= -Ke^{-r(T-t)}N[d_2], \end{aligned} \quad (\text{A.67})$$

where

$$d_2 = \frac{\ln(\frac{S_t}{K}) + (r - \frac{1}{2}\sigma^2)(T - t)}{\sigma\sqrt{T-t}}. \quad (\text{A.68})$$

So, we now must solve  $\pi_{t,s}^1$  of Equation (A.59). The tricky part of this equation is that we cannot move  $S_T$  outside of the expectation like we were able to with  $K$  in solving  $\pi_{t,s}^2$ . However, given that  $B_t = 1$  and  $e^{-r(T-t)} = \frac{1}{e^{r(T-t)}} = \frac{1}{B_T}$ , we can write

$$\frac{\pi_{t,s}^1}{B_t} = \mathbb{E}_{t,s}^{\mathbb{Q}} \left[ \frac{1}{B_T} S_T \chi_{\{S_T \geq K\}} \right]. \quad (\text{A.69})$$

Now, we can change numeraire from  $B$  to  $S$ , giving

$$\frac{\pi_{t,s}^1}{S_t} = \mathbb{E}_{t,s}^{\mathbb{Q}_S} \left[ \frac{1}{S_T} S_T \chi_{\{S_T \geq K\}} \right]. \quad (\text{A.70})$$

The path forward should now be obvious given the steps taken for  $\pi_{t,s}^2$ . We have

$$\begin{aligned} \pi_{t,s}^1 &= S_t \mathbb{E}_{t,s}^{\mathbb{Q}_S} \left[ \chi_{\{S_T \geq K\}} \right] \Leftrightarrow \\ \pi_{t,s}^1 &= S_t \mathbb{Q}_S \left[ S_T \geq K \right], \end{aligned} \quad (\text{A.71})$$

which is analogous now to Equation (A.63), although now under the measure  $\mathbb{Q}_S$ . Using the  $\mathbb{Q}_S$ -dynamics from Equation (A.44), we have

$$\pi_{t,s}^1 = S_t \mathbb{Q}_S \left[ S_t e^{(r + \frac{1}{2}\sigma^2)(T-t) + \sigma W_{T-t}^{\mathbb{Q}_S}} \geq K \right]. \quad (\text{A.72})$$

As before, dividing both sides of the inequality by  $S_t$ , taking logs, and rearranging

$$\pi_{t,s}^1 = S_t \mathbb{Q}_S \left[ \sigma W_{T-t}^{\mathbb{Q}_S} \geq \ln(\frac{K}{S_t}) - (r + \frac{1}{2}\sigma^2)(T-t) \right]. \quad (\text{A.73})$$

Noting that  $\sigma W_{T-t}^{\mathbb{Q}_S} \sim N(0, \sigma^2(T-t))$ , standardizing the random variable as  $\gamma_S = (\sigma W_{T-t}^{\mathbb{Q}_S} - 0)/(\sigma \sqrt{(T-t)})$  and flipping the inequality results in

$$\pi_{t,s}^1 = S_t \mathbb{Q}_S \left[ \gamma_S \leq \frac{\ln(\frac{S_t}{K}) + (r + \frac{1}{2}\sigma^2)(T-t)}{\sigma \sqrt{(T-t)}} \right] \Leftrightarrow \pi_{t,s}^1 = S_t N[d_1], \quad (\text{A.74})$$

where

$$d_1 = \frac{\ln(\frac{S_t}{K}) + (r + \frac{1}{2}\sigma^2)(T-t)}{\sigma \sqrt{(T-t)}}. \quad (\text{A.75})$$

Thus, by Equation (A.61), we have

$$\pi_{t,s} = S_t N[d_1] - K e^{-r(T-t)} N[d_2], \quad (\text{A.76})$$

with

$$d_1 = \frac{\ln(\frac{S_t}{K}) + (r + \frac{1}{2}\sigma^2)(T-t)}{\sigma \sqrt{(T-t)}}, \quad d_2 = \frac{\ln(\frac{S_t}{K}) + (r - \frac{1}{2}\sigma^2)(T-t)}{\sigma \sqrt{(T-t)}}, \quad (\text{A.77})$$

which is the solution to the Black-Scholes equation for a non-dividend paying asset.